

**Titre:** Conversion of D-Xylose to Carboxylic Acids in a Capillary Fluidized Bed

**Auteur:** Touraj Ghaznavi

**Date:** 2014

**Type:** Mémoire ou thèse / Dissertation or Thesis

**Référence:** Ghaznavi, T. (2014). Conversion of D-Xylose to Carboxylic Acids in a Capillary Fluidized Bed [Mémoire de maîtrise, École Polytechnique de Montréal]. PolyPublie. Citation: <https://publications.polymtl.ca/1444/>

## Document en libre accès dans PolyPublie

Open Access document in PolyPublie

**URL de PolyPublie:** <https://publications.polymtl.ca/1444/>  
PolyPublie URL:

**Directeurs de recherche:** Gregory Scott Patience  
Advisors:

**Programme:** Génie chimique  
Program:

UNIVERSITÉ DE MONTRÉAL

CONVERSION OF D-XYLOSE TO CARBOXYLIC ACIDS IN A  
CAPILLARY FLUIDIZED BED

TOURAJ GHAZNAVI

DÉPARTEMENT DE GÉNIE CHIMIQUE

ÉCOLE POLYTECHNIQUE DE MONTRÉAL

MÉMOIRE PRÉSENTÉ EN VUE DE L'OBTENTION  
DU DIPLÔME DE MAÎTRISE ÈS SCIENCES APPLIQUÉES  
(GÉNIE CHIMIQUE)

JUIN 2014

UNIVERSITÉ DE MONTRÉAL

ÉCOLE POLYTECHNIQUE DE MONTRÉAL

Ce mémoire intitulé:

CONVERSION OF D-XYLOSE TO CARBOXYLIC ACIDS IN A  
CAPILLARY FLUIDIZED BED

présenté par : GHAZNAVI Touraj

en vue de l'obtention du diplôme de : Maîtrise ès sciences appliquées

a été dûment accepté par le jury d'examen constitué de :

M. CICOIRA Fabio, Ph.D., président

M. PATIENCE Gregory S., Ph.D., membre et directeur de recherche

M. LEGROS Robert, Ph.D., membre

## DEDICATION

*To my father*

## **ACKNOWLEDGMENTS**

It was a privilege to work with Professor Gregory Patience, he provided me with an opportunity to capitalize on my intrinsic resources to fulfill my ambitions and wishes. I appreciate his continuous support during my program.

During the completion of this research I had an excellent opportunity to work with Dr. Cristian Neagoe, and I learnt many things from him that I will use in all stages of my life. He is someone whom I will never forget.

Thanks to Prof. Fabio Cicoira and Prof. Robert Legros for taking part in my thesis committee.

Dr. Mahdi Jazayeri has helped me a lot over the years, and I consider him a great friend. The support of our research group was also crucial to this work, so I'd to thank all of them.

I would like to thank Mr. Jean Huard, who is part of the technical staff of the Chemical Engineering department, for his support through the experimental setup preparation.

## RÉSUMÉ

La demande pour remplacer les combustibles fossiles par la biomasse renouvelable est grande. Nous recherchons des façons de convertir les glucides en produits de plus grande valeur. Peu d'études ont été faites à haute température et presque aucune expérience n'a examiné l'oxydation partielle catalytique de glucides à haute température. Il nous faut des critères de conception pour exploiter cette technologie de façon commerciale.

Nous présentons une nouvelle méthode de valoriser les sucres C5 et nous faisons une revue de l'état actuel des réactions de sucres C5. Nous voulions développer les conditions optimales pour la production d'acides désirables et éventuellement tester de nouveaux catalyseurs pour d'autres applications.

Nous avons étudié l'oxydation catalytique hétérogène en phase gazeuse du xylose dans un réacteur catalytique de gaz-solide à lit fluidisé capillaire à température relativement haute et à pression atmosphérique. Nous avons oxydé le sucre dans un système à trois catalyseurs, soit le pyrophosphate de vanadyle, le trioxyde de molybdène-oxyde de cobalt et le molybdate de fer, pour former des acides organiques et anhydrides. Nous avons injecté une solution eau-sucre dans un réacteur à lit fluidisé capillaire dont la composante principale était un tube en quartz (ID = 8 mm) dans un four qui opérait jusqu'à 1000 °C. Nous avons déterminé la plage de conditions opératoires avec une étude de reconnaissance et ensuite nous avons préparé un plan d'expérience. Les facteurs les plus importants étaient la température (200–550 °C), la concentration de xylose (3 %<sub>poids</sub>, 7 %<sub>poids</sub>, 10 %<sub>poids</sub> en eau), le temps de séjour (0,1 s, 0,2 s), la pression partielle d'oxygène (0 %<sub>vol</sub>, 3 %<sub>vol</sub>, 10 %<sub>vol</sub>, 21 %<sub>vol</sub> en azote) et le catalyseur (VPP, MoO<sub>3</sub>/CoO, FeMoO). Nous avons co-alimenté l'azote pour améliorer l'atomisation. D'autres paramètres qui affectent l'atomisation sont le rapport gaz-liquide (0,1–0,2 %<sub>poids</sub>), le débit de liquide (0,01–0,1 ml min<sup>-1</sup>) et le diamètre de bout de la buse et du tube capillaire. Nous avions quatre catégories d'atomisation : de 'a', 'b', 'c' et 'd' en ordre décroissant de performance. Nous avons utilisé le type 'a' pour vérifier l'effet des autres paramètres et le type 'b' pour vérifier l'effet de la performance d'atomisation sur le rendement. Nous avons également testé l'alimentation séquentielle de xylose-oxygène et l'air à une fréquence de 5 min<sup>-1</sup>. Pour vérifier la productivité des catalyseurs, nous avons fait des expériences de 2 h et 4 h.

Le temps de séjour dans le lit catalytique était de 0.2 s et les expériences duraient 4 h. Le gaz de fluidisation contenait 3 %<sub>vol</sub> et 10 %<sub>vol</sub> d'oxygène en azote et entrait dans le réacteur par un distributeur en verre fritté. Le débit d'entrée du gaz de fluidisation variait entre 80–150 ml min<sup>-1</sup> pour avoir une pression partielle de l'oxygène de 3 %<sub>vol</sub> et 10 %<sub>vol</sub>. Nous avons fait les expériences avec 1 g de catalyseur VPP calciné. Une pompe à seringue a alimenté la solution de xylose à 0.04 ml min<sup>-1</sup>. Nous avons atomisé le liquide en gouttelettes par un tube capillaire de 0.25 mm serré à l'extrémité de la buse. Nous avons alimenté l'azote et la solution liquide avec un rapport gaz-liquide de 0.18 % <sub>poids</sub> pour produire un jet effervescent. Les gouttelettes se sont vaporisées rapidement et le xylose a réagit pour former de l'anhydride maléique, de l'acide acrylique et de l'acroléine.

Une série de trempes ont absorbé les produits liquides (les acides) de l'effluent du réacteur en eau distillée. Nous avons échantillonné et analysé les acides accumulés par HPLC hors ligne. Pour valider l'analyse par HPLC et pour identifier d'autres produits possibles, nous avons analysé les liquides par chromatographie gazeuse (GC).

Les conditions d'opération ont un effet sur la distribution des produits et les taux de production. L'acide acrylique est le plus désirable et l'acide maléique est le plus abondant. Le pyrophosphate de vanadyl est actif et sélectif dans ce procédé. Dans le meilleur cas, à 300 °C et 10 %<sub>vol</sub> d'oxygène, les rendements de l'acide maléique, de l'acide acrylique et de l'acroléine étaient de 25 %, 17 % et 11 % respectivement. Nous avons détecté du CO<sub>2</sub> gazeux par GCMS lors de la réaction. L'analyse thermogravimétrique des échantillons VPP a confirmé qu'aucun coke ne s'est formé sur le catalyseur. L'agglomération et la caramélation de la poudre n'étaient problématiques que lors de réactions hors de la plage de conditions d'opération établies plus haut.

## ABSTRACT

The demand for renewable biomass as a replacement for fossil fuels has never been greater. Many paths to convert carbohydrates into higher value products are under investigation. Few studies have reported data at high temperature and almost no experiments have examined high temperature catalytic partial oxidation of carbohydrates. We need generalized design criteria to exploit this technology commercially.

We present a new method to valorize C5 sugars and review state of the art C5 sugar reactions. We wanted to develop optimal process conditions to produce desirable acids and eventually to test new catalysts for other applications.

We studied the gas phase heterogeneous catalytic oxidation of xylose in a gas-solid catalytic capillary fluidized bed reactor at relatively high temperature and atmospheric pressure. We oxidized the sugar over three catalyst system (vanadyl pyrophosphate, molybdenum trioxide-cobalt oxide and iron molybdate) to form organic acids/anhydrides. We injected a water-sugar solution into a capillary fluidized bed reactor whose main component is a quartz tube (ID = 8 mm) in a furnace that operates at up to 1000 °C. We determine the range of possible operating conditions with a scouting study and then made an experimental design. The most important factors were temperature (200-550 °C), xylose concentration (3 %<sub>wt</sub>, 7 %<sub>wt</sub>, 10 %<sub>wt</sub> in water), residence time (0.1 s, 0.2 s), oxygen partial pressure (0 %<sub>vol</sub>, 3 %<sub>vol</sub>, 10 %<sub>vol</sub>, 21 %<sub>vol</sub> in nitrogen), and catalyst (VPP, MoO<sub>3</sub>/CoO, FeMoO). Co-feeding nitrogen improved atomization. Parameters that affected atomization are gas-to-liquid ratio (0.1-0.2 %<sub>wt</sub>), liquid flow rate (0.01-0.1 ml min<sup>-1</sup>), and nozzle tip and capillary tube diameter. We had four categories of spray performance: 'a', 'b', 'c' and 'd' in decreasing order of performance. We used a mixed design of experiments including two factors: four temperatures (300 °C, 350 °C, 400 °C, 450 °C) and two oxygen partial pressures (3 %<sub>vol</sub>, 10 %<sub>vol</sub>) with VPP catalyst. We used type 'a' atomization to verify the effect of other parameters and type 'b' to verify the effect of atomization performance on yield. We also tested sequentially feeding of xylose-oxygen followed by air at a frequency of 5 min<sup>-1</sup>. The experimental plan included 2 h and 4 h runs to test catalyst stability.

Residence time inside the catalytic bed was 0.2 s and experiments lasted 4 h. The fluidization gas contained 3 %<sub>vol</sub> and 10 %<sub>vol</sub> oxygen in nitrogen and entered the reactor through a fritted glass distributor. The inlet fluidizing gas stream varied between 80-150 ml/min to meet 3 %<sub>vol</sub> and 10

$\text{\%}_{\text{vol}}$  oxygen. We carried out most experiments with 1 g of calcined VPP catalyst. We metered the 3  $\text{\%}_{\text{wt}}$  xylose solution at 0.04 ml  $\text{min}^{-1}$  with a syringe pump. We atomized the liquid into small drops through a 0.25 mm capillary tube constricted at the end nozzle. We fed nitrogen and the liquid solution with the gas-to-liquid ratio of 0.18  $\text{\%}_{\text{wt}}$  to produce an effervescent spray. The droplets vapourized rapidly and the xylose reacted to form maleic anhydride, acrylic acid and acrolein.

We absorbed the liquid products (acids) from the reactor effluent in distilled water in a series of quenches. We sampled and analyzed the accumulated acids offline with high performance liquid chromatography (HPLC). We validated the HPLC analysis with gas chromatography (GC) and tried to identify other possible products.

Operating conditions have a considerable effect on product distribution and production rates. Acrylic acid was the most desirable and maleic acid the most abundant. Vanadyl pyrophosphate is both active and selective for this process and in the best case, at 300  $^{\circ}\text{C}$  and 10  $\text{\%}_{\text{vol}}$  oxygen, maleic acid, acrylic acid and acrolein yields were 25 %, 17 % and 11 %, respectively. We also detected gaseous carbon dioxide with GCMS during the reaction. Thermogravimetric analysis for the VPP samples we withdrew at the end of the reaction confirmed that no coke formed on the catalyst. Powder agglomeration and caramelization were only problematic when the reactor operated outside the range established during the scouting experiments.

## TABLE OF CONTENTS

DEDICATION .....	III
ACKNOWLEDGMENTS.....	IV
RÉSUMÉ.....	V
ABSTRACT .....	VII
TABLE OF CONTENTS .....	IX
LIST OF TABLES .....	XII
LIST OF FIGURES.....	XIII
NOMENCLATURE.....	XV
CHAPTER 1 INTRODUCTION AND OBJECTIVES .....	1
1.1    Introduction .....	1
1.2    Objectives .....	2
1.2.1    Main objectives .....	2
1.2.2    Specific objectives.....	3
CHAPTER 2 LITERATURE REVIEW .....	4
2.1    Biomass .....	4
2.2    Xylose.....	8
2.3    Current processes.....	10
2.3.1    Biological processes .....	13
2.3.2    Thermo-chemical processes .....	14
2.4    Organic acids .....	17
2.5    Heterogeneous catalysis .....	19
2.6    Fluidized bed reactor .....	20
2.6.1    Fluidized bed principals .....	20

2.6.2 Applications in industry .....	23
2.7 Spray atomization .....	25
2.7.1 Mechanism of atomization .....	25
2.7.2 Applications in catalytic processes .....	28
CHAPTER 3 ORGANIZATION OF THESIS .....	30
3.1 Original scientific hypotheses .....	30
3.2 Methodology .....	30
3.3 Article .....	31
CHAPTER 4 ARTICLE 1 : PARTIAL OXIDATION OF D-XYLOSE TO MALEIC ANHYDRIDE AND ACRYLIC ACID OVER VANADYL PYROPHOSPHATE .....	32
4.1 Presentation of the article .....	32
4.2 Abstract .....	33
4.3 Introduction .....	33
4.4 Experimental .....	36
4.4.1 Catalyst .....	36
4.4.2 Capillary fluidized bed reactor .....	38
4.5 Results and discussion .....	41
4.5.1 Atomization .....	46
4.5.2 Coke formation .....	50
4.6 Conclusions .....	52
4.7 Acknowledgments .....	52
4.8 References .....	52
CHAPTER 5 GENERAL DISCUSSIONS AND PERSPECTIVE .....	55
CHAPTER 6 CONCLUSION AND RECOMMENDATIONS .....	57
6.1 Conclusions .....	57

6.2 Recommendations .....	57
REFERENCES .....	59
APPENDICES .....	68
Appendix A .....	68
Appendix B .....	71

**LIST OF TABLES**

Table 2-1: Typical composition of North American woods (Biermann, 1996) .....	9
Table 2-2: Commercial catalytic fluidized beds (Patience, G.S., 2013) .....	24
Table 4-1: Acid selectivity as a function of operation conditions.....	43

## LIST OF FIGURES

Figure 2-1: Oil refinery versus biorefinery (Kamm et al., 2007) .....	5
Figure 2-2: Two platforms of the concept biorefinery (National Renewable Energy Laboratory) .....	6
Figure 2-3: Identified products from biomass (Werpy et al., 2004) .....	7
Figure 2-4: Structure of xylose; (a) acyclic form, (b) cyclic form .....	9
Figure 2-5: Composition of lignocellulosic biomass (a), composition of various sugars in softwood (b), composition of various sugars in hardwood (c).....	10
Figure 2-6: Processes for converting biomass to energy.....	11
Figure 2-7: Products from xylose .....	12
Figure 2-8: Fluidized bed reactor (Kunii & Levenspiel, 1969).....	21
Figure 2-9: Fluidization regimes .....	21
Figure 2-10: Typical diagram of pressure drop versus gas velocity (Kunii & Levenspiel, 1969).....	22
Figure 2-11: Geldart classification (Geldart, 1973) .....	23
Figure 2-12: Stable satellite (Vassallo & Ashgriz, 1991) .....	25
Figure 2-13: Variables in effervescent atomization (Sovani et al., 2001).....	26
Figure 2-14: Two-fluid injectors; I) externally mixed, II) internally mixed .....	27
Figure 2-15: Electrospray mechanism (Sultan, Ashgriz, Guildenbecher, & Sojka, 2011) .....	28
Figure 2-16: Schematic of electrospray with circle shape ground electrode .....	28
Figure 2-17: Particle characteristics critical - porous vs. non-porous particles (Bruhns & Werther, 2005).....	29
Figure 4-1: Calcined VPP SEM micrographs .....	37
Figure 4-2: EDS trace of calcined VPP catalyst: carbon (C), oxygen (O), vanadium (V), silicon (Si) .....	37
Figure 4-3: VPP XRD pattern: freshly calcined (A), after reaction (A <sub>ox</sub> ), (■) (VO) <sub>2</sub> P <sub>2</sub> O <sub>7</sub> .....	38
Figure 4-4: Experimental system schematic .....	40

Figure 4-5: VPP powder morphology in tests conducted below 300 °C: (a) reactor tube, (b) 1-3 cm above the distributor, (c) 0-1 cm above the distributor .....	41
Figure 4-6: HPLC trace (3 % <sub>wt</sub> xylose, 350 °C and 3 % <sub>vol</sub> O <sub>2</sub> ).....	42
Figure 4-7: Product yield as a function of temperature and oxygen .....	44
Figure 4-8: VPP agglomeration with 7 % <sub>wt</sub> xylose .....	45
Figure 4-9: MoO <sub>3</sub> /CoO powder morphology in tests conducted at 300 °C: (a) 1-3 cm above the distributor (second zone), (b) 0-1 cm above the distributor (first zone) .....	46
Figure 4-10: Atomization types in ambient (a, b, c and d) and their effect on VPP catalyst agglomeration at the nozzle tip (a', b', c' and d').....	48
Figure 4-11: Effect of atomization on product yield for experiments with 3 % <sub>vol</sub> O <sub>2</sub> with VPP catalyst.....	49
Figure 4-12: VPP TGA with air .....	51
Figure 4-13: VPP TGA with N <sub>2</sub> .....	51

## NOMENCLATURE

### English Letters

$d_p$	Particle size
$D_t$	Reactor diameter
$g$	Gravitational acceleration (9.8)
Re	Reynolds number
$U_{mf}$	minimum fluidization velocity
$U_{mb}$	minimum bubbling velocity
$U_t$	maximum gas velocity

### Greek Letters

$\mu$	Gas viscosity
$\Delta p$	Pressure differential
$\rho_s$	Solid density
$\rho_g$	Gas density
$\varepsilon_{mf}$	Porosity at minimum fluidization

### List of Abbreviations

APR	Aqueous Phase Reforming
ALR	Air-to-liquid ratio

## CHAPTER 1 INTRODUCTION AND OBJECTIVES

### 1.1 Introduction

Today, almost all chemicals and polymers are derived from petroleum-based fuels. With petroleum resources that are becoming more difficult to extract and expensive to produce, many research programs have been put in place in the last several years to synthesize chemicals, fuels and energy from renewable biomass feedstock.

Thermal and enzymatic processes exploit carbohydrates to produce chemicals. In thermal processes, energy and syngas are the products. Through enzymatic fermentation the end product is alcohols. Fermentation processes for pentose sugars are extremely rare even though they constitute a high percentage of biomass. Another challenge to ferment biomass is the high percentage of pentose in the hemicellulose, such as xylose, or wood sugar. Unlike hexose (glucose), pentose is difficult to ferment. The economics of these processes are improving with new strains of enzymes resulting in improved yields but the maximum carbon yields are low.

Since C6 sugars are converted to ethanol via fermentation, most of the biological approaches are aiming to supply biofuels for transportation use, an activity which receives a lot of incentives through the renewable portfolio standards in the United States. However, the best C6 sugars sources often happen to be edible sources and a debate of food versus fuels has arisen, jeopardizing a burgeoning but fragile industry mostly based on corn as a feedstock (BiofuelsDigest). Second generation biofuels will rely on other non-edible biomass as feedstock (switchgrass, willow, agriculture residues, municipal solid wastes (MSW), etc.) but the most advanced of these technologies are only reaching the industrial stage.

Gas-solids heterogeneous catalysis offers the potential to open up new routes to producing highly valued chemicals while reducing the number of process steps. Liquid-solids heterogeneous catalysis has been practiced for many years (Hattori et al., 1978). However, mass transfer limitations, low reaction rates and separating catalyst from the product are some of the common limitations of this technology. These limitations may be minimized by operating in the gas phase vaporizing the liquid and simultaneously contacting it with a catalyst powder. Vaporizing carbohydrates starch, mono-saccharides, di-saccharides, etc. can be difficult. Furthermore, these compounds caramelize at temperatures below 200 °C. Mass transfer and selective reaction rates

may be enhanced by vaporizing a liquid solution of the carbohydrates and simultaneously contacting it with a solid catalyst. Vaporizing carbohydrates can be difficult due to the kinetics of caramelization. When heated, sugars will decompose readily and becoming highly cohesive. In the proposed technology, we feed a liquid solution containing carbohydrates (pentose, for example) through a nozzle that forms a spray directly inside a fluidized bed of catalyst particles. The droplets from the spray vapourize rapidly and then react with the solid catalyst. The vaporization and reaction rates are superior to the decomposition rate thus we minimize yield losses due to caramelization.

Typically, caramelization, which comprises scissions, molecular rearrangement, and subsequent reactions, occurs at temperatures as low as 154 °C. However, many heterogeneous catalytic oxidation reactions take place at temperatures exceeding 300 °C. Increasing the temperature of sugar solutions to these high reaction temperatures results in significant yield losses. Moreover, heating the solution could cause severe operational difficulties: line blockage, deposition, coking etc.

The fluidized bed reactor combines the advantage of high yields and reaction kinetics associated with a thermo-chemical approach without some of its undermining characteristics because the reactions are performed at a lower temperature. As for the present technology, it has over the biological approach the advantage of rapidly converting in one reaction pass the C5 sugars (xylose) into valuable chemicals.

The present technology (Patience, G., Shekari, & Farrie, 2013) positions itself as a mean to produce higher value green chemicals. Among the products, the preferred chemical is acrylic acid, because of its large respective user base.

## **1.2 Objectives**

### **1.2.1 Main objectives**

Based on the several potential reaction pathways proposed by literature to implement in a forest biorefinery and their identified technical problems, the applications and possible commercial possibility of current work are in biomass conversion, polymer industry and chemical additives.

The potential commercial benefits will be relatively low cost production of organic acids. The main objective of the current project is to convert xylose to value added chemicals with high yield.

### **1.2.2 Specific objectives**

The objective of this research project is to develop process technology to produce organic acids by catalytic conversion of C5 (pentose) sugars in a fluidized bed reactor. In our preliminary experiments, we have succeeded to produce a range of valuable organic acids by oxidation of xylose (pentose) over vanadyl pyrophosphate (VPP) catalyst in a fluidized bed.

We have, thus far, demonstrated that the conversion of xylose to various organic carboxylic acids can be achieved by selecting the proper catalysts and conditions, which could provide a renewable platform for the chemical industry.

- Partially oxidize xylose over metal oxide catalysts in a micro-fluidized bed reactor.
- Establish optimal process conditions to produce acids and identify a catalyst that maximizes yield.
- Identify spray nozzle conditions to avoid xylose from caramelizing at the nozzle or agglomerate the catalyst.

The strength of the present work is therefore its capacity to address a need for greener sources of feedstock to produce chemical commodities at costs that are similar to existing petroleum-based products.

## CHAPTER 2 LITERATURE REVIEW

### 2.1 Biomass

A long term solution of the finite resource of fossil-fuel resources is to direct technology to change feedstock for chemical industries. Starting materials and feedstocks are essential part of design for sustainability. This means that any successful future design must use raw materials that are renewables rather than depleting. Organic wastes and biomass are major sources of non-fossil carbon source to produce chemicals.

Sustainable economic development requires safe and sustainable resources for industrial production. For sustainable economic growth, the utilization of non-renewable raw material should be reduced. An approach is to replace gradually the global economy from fossil based into bio based sustainable economy. The fundamental of this economy will be on production of bioenergy, biofuels and bio products.

In addition to the growing price and supply uncertainties, current industries suffer from high level of environmental emissions due to the operating process and raw materials. Emission of toxic materials during petrochemical processes is high. Whereas, the processes with production of liquid fuels and organic chemicals from biomass resources don't have such emissions.

Biomass is a renewable natural feedstock with minimum environmental concerns. But there are still technical obstacles in commercializing the methods for production of chemicals and energy from this material. Lots of research and development is required to develop the knowledge of biomass conversion. First-generation of biofuels derives from plants and fermentation of sugars. Biodiesel made from vegetable oils take place in the first-generation. In the other hand, second-generation derives from lignocellulosic biomass, goes through biochemical and thermochemical processes (Kamm, Gruber, & Kamm, 2007).

According to Zobelein (2001), biomass includes all living organic materials existing in our ecological system and the plants which are in a continuous renewal by photosynthesis ( $nCO_2 + nH_2O \rightarrow (CH_2O)_n + nO_2$ ) and also the living cellulose of plants, animals and microorganism. According to US government program (Congress, 2000; President, 1999), biomass is an organic renewable material including energy crops, trees, agricultural food and residues, marine plants, wood and wood residues and waste materials .

Using biomass as a feedstock to produce products is relatively new and the main objective is to convert organic materials into valued products using a combination of technologies and biotechnological processes. A comparison between basic principles of petroleum refinery and future biorefinery products is in Figure 2-1.

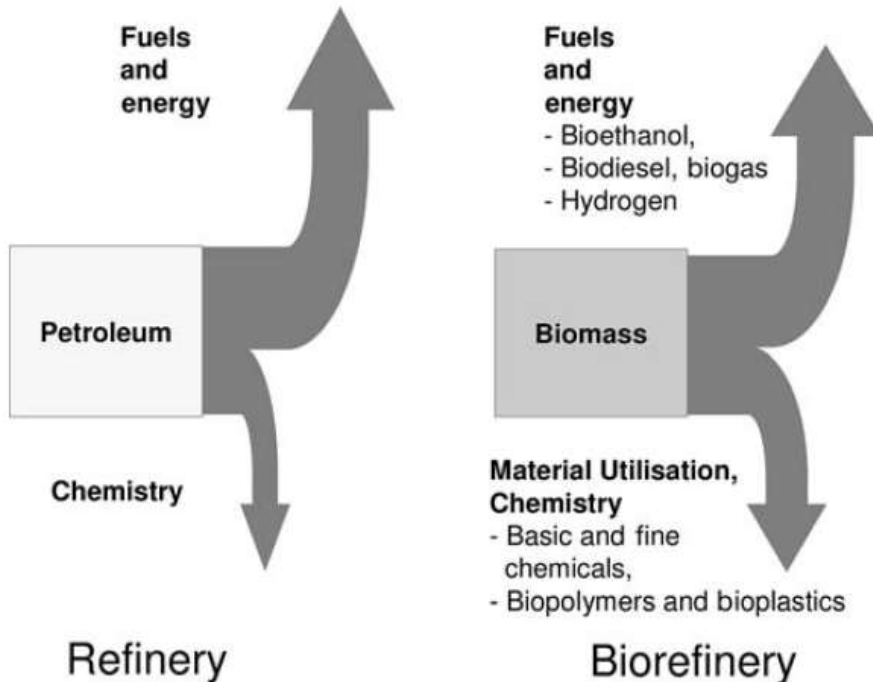


Figure 2-1: Oil refinery versus biorefinery (Kamm et al., 2007)

The use of lignocellulosic biomass within the context of the biorefinery is based on two different platforms (Pereira, Couto, & Santa Anna, 2008); sugar platform based on biochemical conversion and syngas platform known as thermochemical platform. The concept of these two platforms (TPCBR) biorefineries is in Figure 2-2.

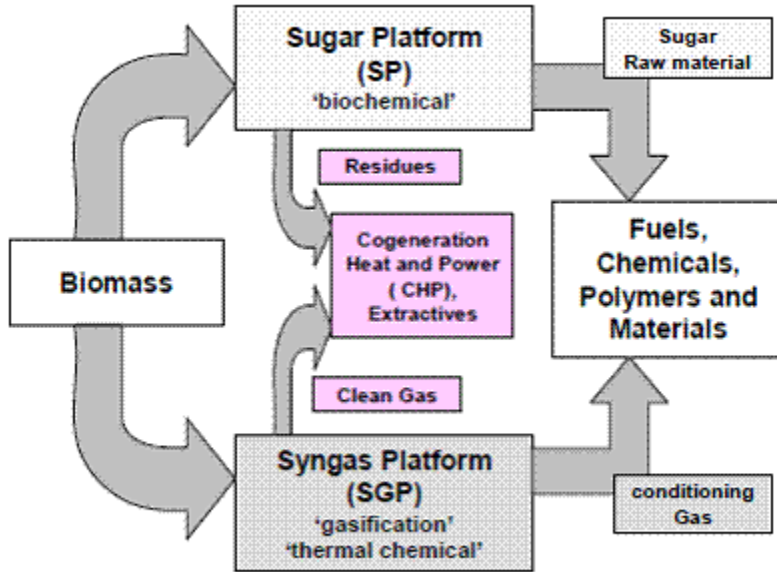


Figure 2-2: Two platforms of the concept biorefinery (National Renewable Energy Laboratory)

Carbohydrates, lignin, proteins, fats and verity of substance are the basic component of biomass. According to Kamm et al. (2007) 75% of biomass is carbohydrate, 20% lignin and only 5% other natural compounds, which means carbohydrates are important representative for converting to chemicals. According to Pacific Northwest Laboratory and National Renewable Energy laboratory (Werpy et al., 2004) top potential biobased chemicals from sugars by chemical and biological pathways are: 1,4-diacids (succinic, fumaric and maleic), 2,5-furan dicarboxylic acid, 3-hydroxy propionic acid, aspartic acid, glucaric acid, glutamic acid, itaconic acid, 3-hydroxybutyrolactone, glycerol, sorbitol and xylitol/arabinitol. The studies of these potential chemicals included precursors, platforms, building blocks, secondary chemicals, intermediates and products and uses (Fig. 2-3).

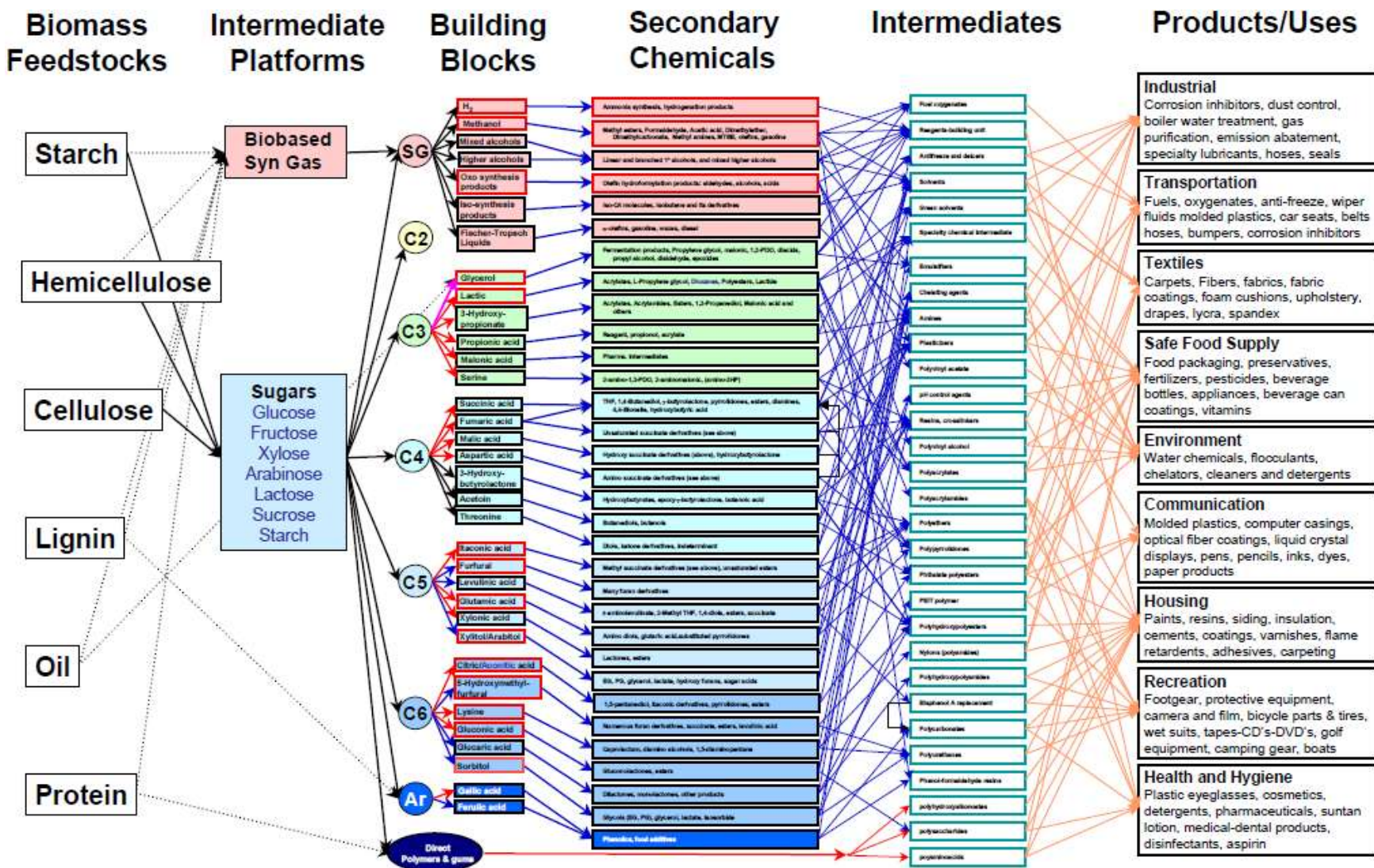


Figure 2-3: Identified products from biomass (Werpy et al., 2004)

## 2.2 Xylose

Lignocellulosic biomass is a low-cost source and most abundant continuously renewable material and consists of carbohydrate polymers (cellulose and hemicellulose) and aromatic polymers (lignin). This composite forms the body of wood. Hard wood lignocellulose is approximately 40-50% cellulose, 25-35% hemicellulose and 20-25% lignin (Fengel & Grosser, 1975). It has been used for:

- Paper and pulp production from wood
- Soluble cellulose derivatives, viscose and other cellulose based synthetic fibers
- Wood-based sugar production and wood liquefaction
- Vanillin production from lignin
- Nitration of cellulose (guncotton and nitro rayon)
- Furfural and nylon

Hemicellulose is the third most abundant polymer in nature and includes xylan, glucuronoxylan, arabinoxylan, glucomannan, and xyloglucan. Hydrolysis of these soluble polysaccharides forms simple sugars. Hemicellulose contains mostly D sugars and a small amount of L sugars of which D-xylose is the most abundant.

Carbohydrates, being the most abundant class of biomolecules, are distributed widely in nature. Monosaccharides, disaccharides and polysaccharides (or oligosaccharides) are classified as carbohydrates. Monosaccharides are classified based on the nature of the carbonyl groups known as aldoses and ketoses in which an aldose contains an aldehyde ( $\text{CH}=\text{O}$ ) group and a ketose contains ketone ( $\text{C}=\text{O}$ ) groups. The number of C's in the monosaccharide indicated by the roots: tri-, tetra-, penta-, hexa- and after the root the -ose suffix designates a carbohydrate. As an example of aldopentose is xylose.

Wood is primarily composed of cellulose, hemicellulose, lignin, extractive substances and ash. A typical wood's chemical composition is in Table 2-1 (Miller M., 2005).

Table 2-1: Typical composition of North American woods (Biermann, 1996)

Compound	Hardwoods	Softwoods
Cellulose	40-50	45-50
Hemicellulose	17-35	25-35
Lignin	18-25	25-35
Extractive	1-5	3-8
Ash	0.4-0.8	0.2-0.5

Xylose, a five carbon carbohydrate, is the second most abundant sugar on earth after glucose. Xylose is available in both L and D forms and the L form is relatively expensive. Xylose has two structures, acyclic and cyclic (Fig. 2-4) (Brown, 1961). Figure 2-5 shows the composition of lignocellulosic biomass and the percentage of xylose among biomass feed stocks of which the fraction of d-xylose in hardwood is much higher than in softwoods (Casey, 1980). The major raw materials to produce xylose with 98% purity include a mix of hardwoods birch and beech, and corn cobs used for the production of xylose with 99% purity. A high amount of C5 sugars is present in agricultural residues (Singh, A. & Mishra, 1995).

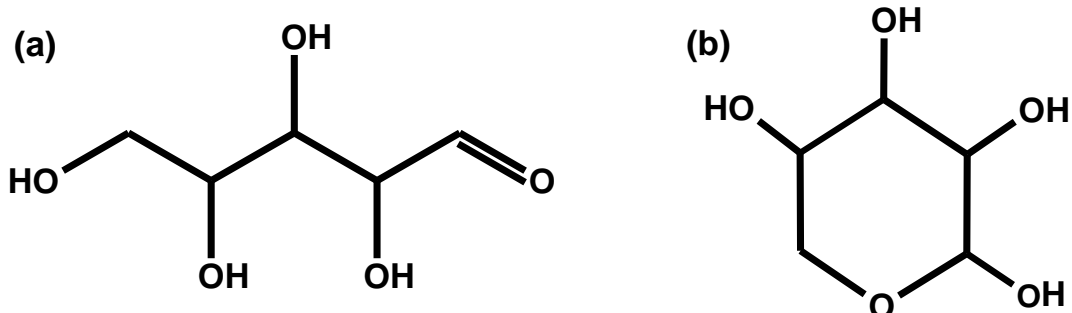


Figure 2-4: Structure of xylose; (a) acyclic form, (b) cyclic form

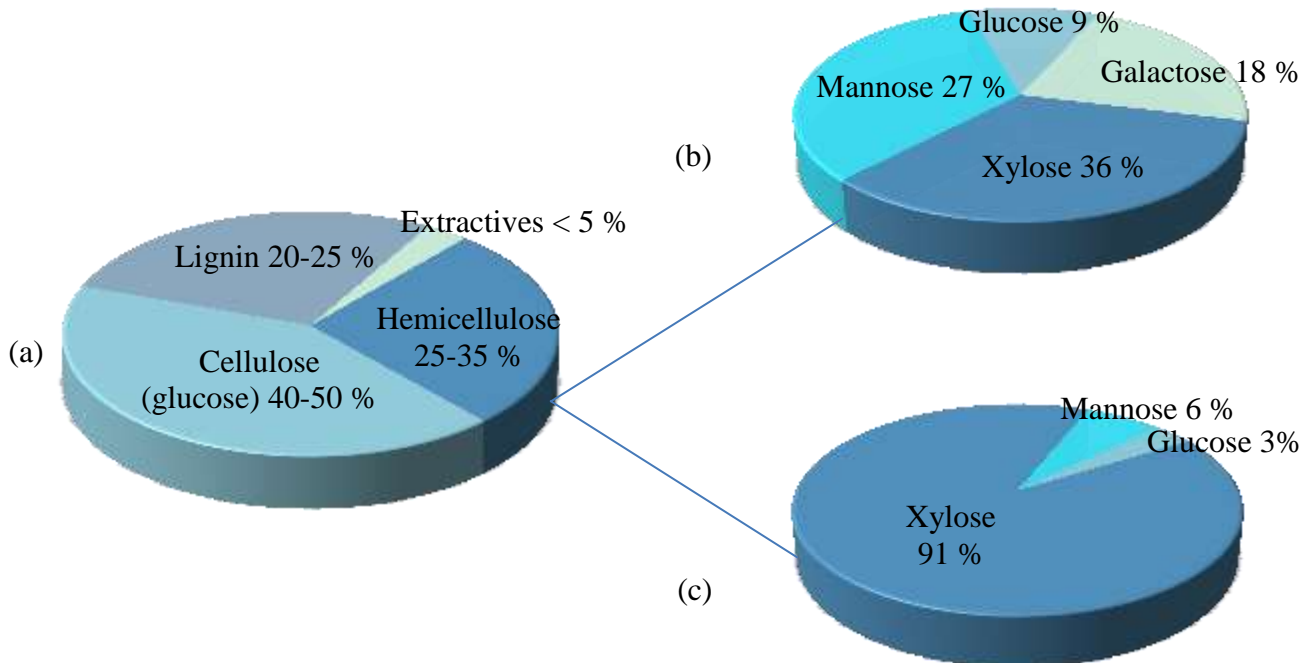


Figure 2-5: Composition of lignocellulosic biomass (a), composition of various sugars in softwood (b), composition of various sugars in hardwood (c)

## 2.3 Current processes

There are many investigations to convert sugars to chemical. Most current applications of hemicellulose products are limited to low technology applications such as to generate energy for pulp mills, to produce adhesives for chip boards and to ferment to ethanol. Other processes are some pathways with some more efficient processes for hemicellulose isolation is higher temperatures or pressures in extraction process. Low yield in enzymatic fermentation of pentoses to ethanol, economical matters in conversion of mannose to products are examples of problems with hemicellulose conversion.

Different biochemical and thermo-chemical routes are used to breakdown sugars into simple molecules. To convert the biomass feedstock into alcohols, chemicals and energy, two main

approaches are used, the biological (fermentation) and the thermo-chemical (gasification, pyrolysis and combustion) approaches (Figs. 2-6,-7).

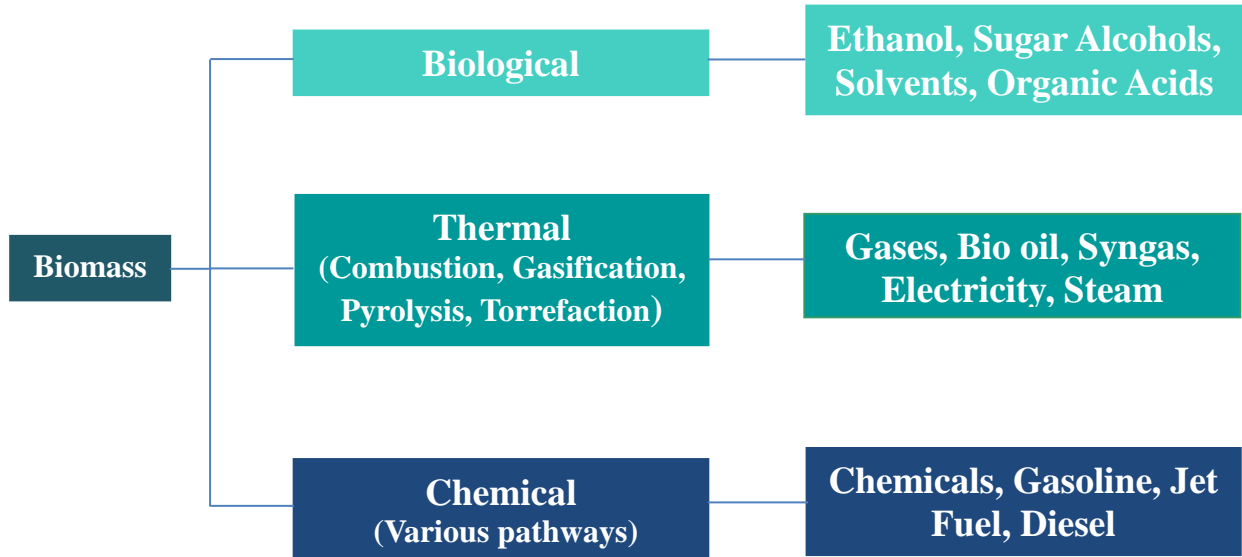


Figure 2-6: Processes for converting biomass to energy

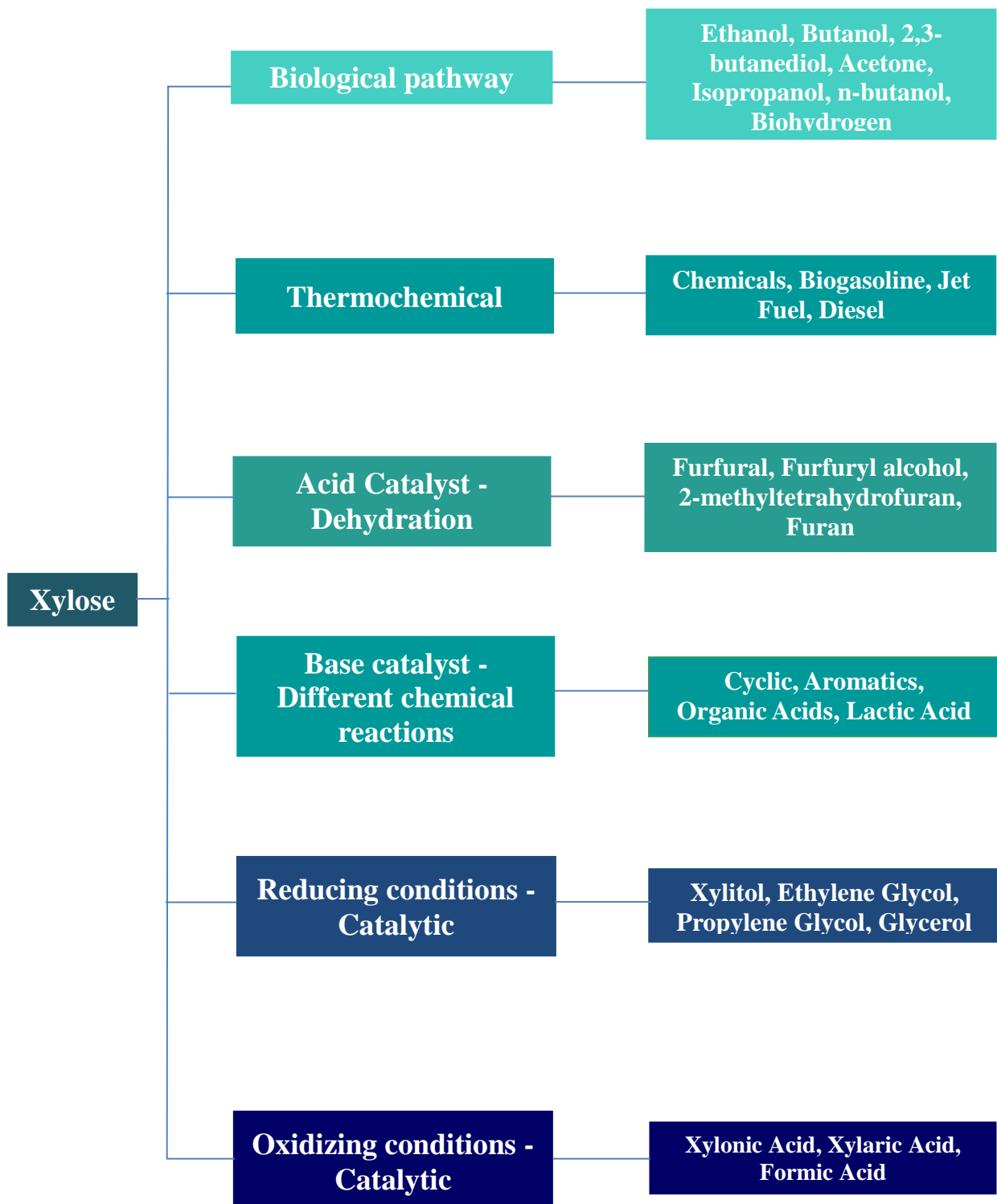


Figure 2-7: Products from xylose

### 2.3.1 Biological processes

Sugars can convert to various products such as ethanol, sugar alcohols, solvents and organic acids, by microorganisms. Biological conversion of d-xylose can produce ethanol, butanol, 2,3-butanediol, acetone, isopropanol and n-butanol (Beall, Ohta, & Ingram, 1991; Lachke, 2002; Singh, A. & Mishra, 1995).

In enzymatic processes (fermentation) ethanol is the target molecule to be blended with petroleum (Singh, A. & Mishra, 1995). However, this route is uneconomic due to the high feedstock cost, enzyme cost, pretreatment cost, and fermentation cost. Moreover, the maximum carbon yields are relatively low (Himmel, Vinzant, Bower, & Jechura, 2005). As for the biological approach, yields are improving with recent developments and even xylose (C5), can now be converted to alcohol. There are plants in Europe producing ethanol (e.g. Borregaard in Norway) and the ABE process, producing acetone, butanol and ethanol is working well on C5 sugars since the Clostridia Acetobutylicum that tolerates well these sugars. The main limitation for biotechnologies is that C5 sugars (in hemicellulose) are fermentation inhibitors in many processes, and that hydrolysis processes generate additional fermentation inhibitors such as acetic and formic acids, but also furfuraldehyde and others. This is the reason why “food-grade” sugars are used so far in fermentation technologies. A chemical process will be much more tolerant to these fermentation inhibitors, but will suffer from other impurities like salts or low temperature stability and need to be designed to cope with these difficulties.

In some metabolic pathways, bacteria go through direct xylose to xylulose conversion via isomerization (Lachke, 2002). Trillium FiberFuels (Beatty, Potochnik, & Pease, 2009) invented a process that converts xylose to ethanol in two steps: first xylose isomerizes to xylulose then the xylulose ferments to ethanol using *Schizosaccharomyces Pombe* yeast. However, the economics are poor.

Microorganisms produce hydrogen from sugar (Kim, Kim, & Shin, 2009; Levin, Pitt, & Love, 2004). Researchers of Virginia Tech developed an enzyme-driven process to convert xylose into hydrogen at low-temperature (50 °C) and atmospheric-pressure in a reactor containing 13 enzymes, with nearly 100% of the theoretical yield (Martín del Campo et al., 2013).

There are many studies to produce lactic acid from xylose with microbes (Abdel-Rahman, Tashiro, & Sonomoto, 2011; Okano, Tanaka, Ogino, Fukuda, & Kondo, 2010; Yadav, Chaudhari,

& Kothari, 2011). The concept is fermenting carbohydrate-based syrup by lactic acid bacteria (LAB).

Xylose converts to xylonic acid through metabolic pathways (Bernhauer & Riedl-Tumova, 1949; Buchert, Viikari, Linko, & Markkanen, 1986; Hayasida, 1938; Ishizaki, Ihara, J, M, & Imai, 1973), but compared to the production of biofuels or xylitol, there are few published studies with this route.

Using bacterial strains leads to production of xylitol from xylose (Yoshitake, Ohiwa, Shimamura, & Imai, 1971).

### 2.3.2 Thermo-chemical processes

Gasification, pyrolysis, and liquefaction are common thermal processes used to ultimately produce methanol, methane, olefins, diesel, gasoline etc. But these conventional approaches have a number of intermediate steps that jeopardize the potential profitability. Even if the thermo-chemical processes have the advantage of converting almost 100 % of the biomass, the high temperature under which they are performed form carbon oxides resulting in yield losses.

In chemical looping gasification the oxygen is provided indirectly by circulating a metal oxide between a gasifier and oxidizer (Fan, 2011). The produced syngas has a higher calorific value compared to traditional gasification processes. Although the operating cost is lower, the capital cost and oxygen carrier life time are the main issues to be resolved.

Xylosan is formed by the pyrolysis of xylose. It is easily oxidized to furfural. Acetylation of xylosan yields diacetylxylosan (Hurd & Isenhour, 1932). Hydrogenolysis of polyhydroxylated compounds (xylose) over a catalyst yields alcohols, acids, ketones, ethers, and hydrocarbons (Arena, B.J., 1983).

Researchers are developing processes to convert biomass to liquid fuels (Regalbuto, Jun 25 2009) such as catalytic conversion of carbohydrates (Kunkes et al., 2008), conversion of sugars through hydrolysis, dehydration, isomerization, aldol condensation, reforming, hydrogenation, and oxidation in liquid phase to produce chemicals and fuels (Chheda, Huber, & Dumesic, 2007). Aqueous phase hydrodeoxygenation of carbohydrates (xylose) over bifunctional catalysts

involving C-C and C-O bond cleavage and hydrogenation reactions leads to C1– C6 alkanes, C1– C6 primary and secondary alcohols, cyclic ether and polyols (Heracleous & Lemonidou, 2013; Li, Tempsett, & Huber, 2010).

Another indirect competitor that can be seen as an example of a new entrant into the chemical commodities marketplace is Anellotech (Anellotech), a University of Massachusetts spin-off who convert biomass into aromatics. Its business model is to build, own and operate its own plants, a potentially lucrative proposition. Catalytic fast pyrolysis of lignocellulosic biomass in a fluidized bed in the presence of a zeolite-based catalyst forms aromatic and olefinic hydrocarbons along with CO, CO<sub>2</sub>, H<sub>2</sub>O, and undesired coke (Huber, Cheng, Wang, & Fan, 2013; Huber, Zhang, & Carlson, 2013).

Virent Energy Systems uses a fluidized bed reactor to convert biomass to biofuels and is presently at the pilot phase. Cane sugar to Green Gasoline is based on a novel Aqueous Phase Reforming (APR) technology to produce conventional liquid transportation fuels from biomass. Reactions include: reforming to generate hydrogen; dehydrogenation of alcohols/hydrogenation of carbonyls; deoxygenation reactions; hydrogenolysis; and cyclization, converts to mixture of chemical and oxygenated hydrocarbons including alcohols, ketones, acids, furans, paraffins and other oxygenated hydrocarbons. With further catalytic processing, these intermediate compounds react over a Virent modified ZSM-5 catalyst to produce nonoxygenated hydrocarbons, a high-octane gasoline (Blommel, Yuan, Van Straten, Lyman, & Cortright, 2013; Cortright, 2013; Cortright & Blommel, 2013; Kania et al., 2013).

Xylose dehydrates to furfural in the presence of different types of acid catalyst, either Brønsted or Lewis. The temperature is generally between 140-240 °C and the molar conversion is between 53-98% (Fuente-Hernández, Corcos, Beauchet, & Lavoie, 2013) depending on the catalyst. These heterogeneous catalytic processes are very efficient (Bugrayev et al., 2008; Lessard, Morin, Wehrung, Magnin, & Chornet, 2010). Furfural is a solvent but is a primary feedstock for other products: Partial reduction of furfural results in furfuryl alcohol which is used in resins, adhesives and wetting agents. Furfural reduces to 2-methyltetrahydrofuran (Me-THF) which could replace tetrahydrofuran (THF) (Wabnitz, Breuninger, Heimann, Backes, & Pinkos, 2010, 2012). Another challenge is decarboxylation of furfural to furan (Stevens, Bourne, Twigg, & Poliakoff, 2010; Zhang, Zhu, Niu, & Li, 2011).

Xylose reacts to form cyclic compounds (Popoff & Theander, 1976). While most of the products are aromatic, some produce lactic acid (Jackson, Miller, & Marincean, 2008; Johansson & Samuelson, 1977). Epimerisation of xylose gives C6 sugars which 1 % glucose and 2.5 % of sorboserabinose and efficiently to C5 sugars, lylose with 18 % and arabinose with 15 % (El Khadem, Ennifar, & Isbell, 1987).

Since xylose has carbonyl functionality, it is more difficult to be reduced. Xylose reduces to xylitol between 100-125 °C (lower than the melting point of xylose) in the presence of the metal based catalyst such as nickel, ruthenium, rhodium and palladium (Alen et al., 2003; Mikkola, J.-P. & Salmi, 2001; Mikkola, J. P. et al., 2003; Riihimaeki Teppo, 2006; Wisniak, J, Hershkowitz, Leibowitz, & Stein, 1974; Wisniak, Jaime, Hershkowitz, & Stein, 1974). Glycerol, ethylene glycol and propylene glycol can be produced from xylitol at temperatures around 250 °C (Crabtree & Tyers, 2007). Hydrogenolysis of xylitol gives mixtures of polyols and other products such as formic acid and lactic acid produced (Sun & Liu, 2011).

Aldehyde groups are much easier to oxidize than ketones and give carboxylic acids. With a strong oxidizing agent, like  $\text{KClO}_3$ , sugar converts completely to carbon dioxide, which is highly exothermic (Shapley, 2012). Monosaccharides are a source of aldonic acids such as gluconic acid (Japanese patent No. 7620/58) that react over platinum or palladium, under an alkaline condition. Palladium on carbon catalyst with an oxygen carrier gas resulted in high yield<sup>1</sup>. Catalytic oxidation of glucose in the presence of Pt group catalyst and gold on carbon catalysts produces gluconic acid (Comotti, Pina, Matarrese, Rossi, & Siani, 2005; Mallat & Baiker, 2004). Oxidation of xylose in the presence of metallic catalyst is interesting. Using gold, palladium and copper catalyst xylose oxidizes to xylonic acid at temperatures between 25-60 °C (Bonrath & Fischesser, 2010; Prüße, Heidkamp, Decker, Herrmann, & Vorlop, 2010; Van der Weijden, Mahabir, Abbadi, & Reuter, 2002). Trihydroxydiacid and aldaric acids such as xylaric acid also produce by oxidation of xylose (Kiely & Hash, 2008; Venema, Peters, & van Bekkum, 1992). Iodate oxidation of xylose with Ir(III) catalysis gives threonic acid and formic acid (Singh, A. K., Srivastava, Srivastava, & Singh, 2007). Also, oxidation of xylose by acid solution of vanadium (V) in the presence of manganese II as homogeneous catalyst produces formic acid (Odebunmi, Ogunlaja, & Owalude, 2010). Under more severe oxidizing conditions, breakage of the carbon-carbon bonds in the molecule of xylose leads to the production of organic acids such as formic and acetic acid (Isbell, Frush, & Martin, 1973). Using electrotechnologies leads to conversion of

xylose to xylonic acid and xylitol with efficiency of 80 % (Jokic, Ristic, Jaksic, Spasojevic, & Krstajic, 1991). Also, electro-oxidation of d-xylose on platinum and gold catalyst yields carboxylic acids. During electrolysis xylonic acid predominates but glyceric, glycolic and formic acids were also detected (Governo, Proenca, Parpot, Lopes, & Fonseca, 2004).

Molecular oxygen has been used to convert carbohydrates to produce alditols and aldoses (Arena, Blaise J & Schumacher, 1992) and to oxidize glucose to gluconic acid with in the presence of an activated charcoal supported catalyst containing a platinum group metal component in an aqueous alkaline solution (Deller, Despeyroux, Krause, & Peldszus, 1992).

## 2.4 Organic acids

Currently, organic acids such as maleic, acrylic and methacrylic acid are produced by the partial oxidation of fossil based C3 to C4 alkanes and olefins. Among the desired compounds in this project is acrylic acid. Acrylic acid is a monomer for polymers. Commercial processes to acrylic acid rely on propylene as a feedstock although acetylene and propane may become viable alternatives. Some other developing routes use glucose, glycerol and ethylene as feedstock and acetic acid to acrylate esters.

Acrylates are primarily used to prepare emulsion and solution polymers and superabsorbants (polymers) for diapers (Kirk-Othmer Encyclopedia of Chemical Technology (Suslick, 1998)). The emulsion polymerization process provides high yields of polymers in a form suitable for a variety of applications. Acrylate polymer emulsions were first used as coatings for leather in the early 1930s and have found wide utility as coatings, finishes, and binders for leather, textiles, and paper. Acrylate emulsions are used in the preparation of both interior and exterior paints, floor polishes, and adhesives. Solution polymers of acrylates, frequently with minor concentrations of other monomers, are employed in the preparation of industrial coatings. Polymers of acrylic acid can be used as superabsorbents in disposable diapers, as well as in formulation of superior, reduced-phosphate-level detergents. Also, methacrylic acid is used as a raw material for methyl methacrylate (MMA). The methacrylates have numerous uses, most notably in the manufacture of polymers with trade names such as Lucite and Plexiglas. These applications have driven a steady growth between 5% and 6% per annum in worldwide sales.

The major players, based on a new report by Research & Markets are the following:

- Dow Chemical Company (N° 2 in Acrylic Acid)
- Mitsubishi Chemical Corporation
- Evonik Industries AG
- Air Products and Chemicals Inc
- Archer Daniels Midland Company
- Ashland Inc
- BASF (N° 1 in Acrylic Acid)
- Eastman Chemical Company
- INEOS Group
- Lubrizol
- PolyOne Corporation
- Arkema SA (N° 3 in Acrylic Acid, and N° 1 in PolyMethylMethAcrylate, PMMA)
- Celanese Corporation

Worldwide demand for acrylic acid is 5 000 kta. With production units of 100 kta, every new plant based on the proposed invention would contribute to supply 2 % of this demand so there is plenty of room in the marketplace for new production capacity. Moreover, the price for the various declinations of acrylates is ranging historically between \$2000 and \$ 3000 per ton (ICIS). Its value is 5 to 10 times greater than biofuels which makes it an attractive alternative requiring less fewer governmental subsidies/incentives.

Maleic anhydride is commercially produced by oxidation of benzene or butane which the butane-based process has superior economics. Maleic anhydride is used for the manufacturing unsaturated polyester resins for the application of bathroom fixtures and automobiles or a versatile intermediate for producing pharmaceuticals and agrochemicals such a 1,4 butanediol, derivatives tetrahydrofuran and gamma-butyrolactone.

Organic acids could be produced by conversion of biomass. Using Carbohydrate derivatives like; oxidation of furfural and HMF in the presence of a heterogeneous rhenium based catalyst, and a co-catalyst lead to the production of maleic acid, succinic acid, malic acid and fumaric acid and maleic acid can be dehydrated to lead to maleic anhydride (Saladino & Farina, 2013). Using hexoses like, glucose and lactose oxidize to gluconic acid and lactobionic acid using a gold catalyst (Thompson, 2006).

This will be the first time that these chemical will be produced on a commercial scale by the catalytic gas phase conversion of sugar compounds. Huge volumes of acrylic acid are currently

produced from non-renewable petroleum based feedstock. With development of our innovative approach, renewable resources could supply for the immense demand for acrylic acid. Moreover, it is estimated that due to its lower unit price, sugar feedstock would lead to cheaper production of acrylic acid as opposed to petroleum based process.

## 2.5 Heterogeneous catalysis

Current studies are mainly concerned with high pressure liquid phase catalytic oxidation, hydrogenation or hydrolysis of sugars to organic acids and polyalcohols. Among the emerging technologies, those based on catalysis have been identified as a potential to produce functionalized molecules with a higher value add compared to fuel. Activities are ongoing to render catalytic processes cost effective on a large scale. Gas-solids heterogeneous catalysis has the potential to produce valued chemicals with fewer process steps (Oh-Kita & Kita, 1988).

Vanadium containing catalyst systems are used in mild oxidation, ammoxidation and dehydrogenation of hydrocarbons and other organic compounds (Courtine & Bordes, 1997) with industrial reaction of; o-xylene to phthalic anhydride and benzene to maleic anhydride (Bielański, Piwowarczyk, & Poźniczek, 1988; Grzybowska, 1987; Nikolov, Klissurski, & Anastasov, 1991; Védrine, 1994; Wainwright & Foster, 1979). VPO oxidize alkanes to maleic anhydride (Bergman & Frisch, 1966) or adding promoter for this mix oxide catalyst (Jurewicz, Weinstein, & Young, 1975; Kerr, 1964). The VPO catalyst is both active and selective for this process (Batis, Batis, Ghorbel, Védrine, & Volta, 1991; Benabdelouahab, Volta, & Olier, 1994; Bordes, 1987, 1988, 1993; Bordes & Courtine, 1979; Centi, G., 1993; Centi, Gabriele, Trifiro, Ebner, & Franchetti, 1988; Contractor, R. M. et al., 1988; Hodnett, 1987; Pepera et al., 1985; Trifirò, 1993; Ziolkowski, Bordes, & Courtine, 1990).

With respect to the catalyst, vanadyl pyrophosphate (VPP) has shown various functionalities in oxidation and dehydration for formation of C4 olefins or dienes, furan, acetic, acrylic and maleic acids as well as methacrolein. Based on these observations, VPP is a multifunctional catalyst that can isomerize, dehydrogenate, dehydrate and oxidize organic substrates. The mean oxidation state of vanadium is between  $V^{4.0+}$  and  $V^{5.0+}$  (Courtine & Bordes, 1997). The catalyst has strong acid sites, both Brønsted and Lewis (Busca, Centi, Trifiro, & Lorenzelli, 1986; Centi, G,

Golinelli, & Busca, 1990; Cornaglia, Lombardo, Andersen, & Fierro, 1993) which plays a key role in the reaction as an electron accepter (Lewis) and proton donor (Brønsted).

VPP catalyst was specifically designed by DuPont (Patience, Gregory S & Bordes-Richard, 2010) to convert n-butane to maleic anhydride in a circulating fluidized bed reactor (CFBR). The VPP catalyst consists of vanadium (V), phosphorus (P) and oxygen (O). For the catalyst synthesis, vanadium pentoxide ( $V_2O_5$ ) was refluxed in a solution of isobutyl and benzyl alcohol and phosphoric acid ( $H_3PO_4$ ) (85%) with P/V ratio of 1.0 to form vanadyl phosphate hemihydrate ( $VOHPO_4 \cdot H_2O$ ) crystals 70  $\mu m$  in diameter. After drying, the precursor was milled to 2 to 2.5  $\mu m$  then slurried with polysilicic acid (5-10 %<sub>wt</sub>). The Sauter mean diameter of the microspheres from the spray dryer was from 70 to 80  $\mu m$ . It was calcined in the commercial regenerator at 390 °C and formed vanadyl pyrophosphate –  $(VO)_2P_2O_7$  (Patience, Gregory S, Bockrath, Sullivan, & Horowitz, 2007).

Two other catalyst systems; molybdenum trioxide-cobalt oxide (supplied by Arkema) and iron molybdate (prepared by Haldor Topsøe) (Rase, 2000; Soares, Portela, & Kienemann, 2005) were tested. Other catalyst systems that could be interesting for this process include transition metals such as Fe, Cu, Pt, Pd and Ni or their metal oxides supported over alumina, silica or zeolites or a variety of mixed metal oxides.

## 2.6 Fluidized bed reactor

### 2.6.1 Fluidized bed principals

In a fluidized bed, solid powders are suspended by an upward flowing fluid stream (Fig. 2-8). This type of reactor has the ability to process large volumes of fluid with excellent gas-solid contacting, high heat and mass transfer rates between gas and particles without any hot spot even for highly exothermic reactions.

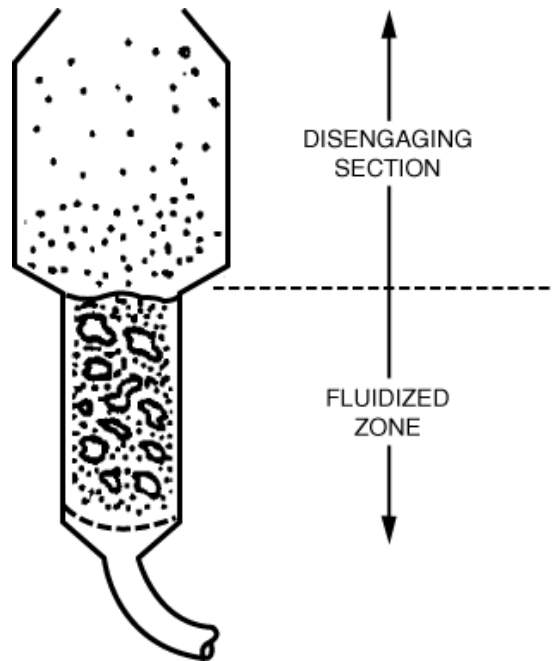


Figure 2-8: Fluidized bed reactor (Kunii & Levenspiel, 1969)

Operation conditions in the reactor such as; gas velocity and gas and solid properties changes the fluidization behavior (Fig. 2-9).

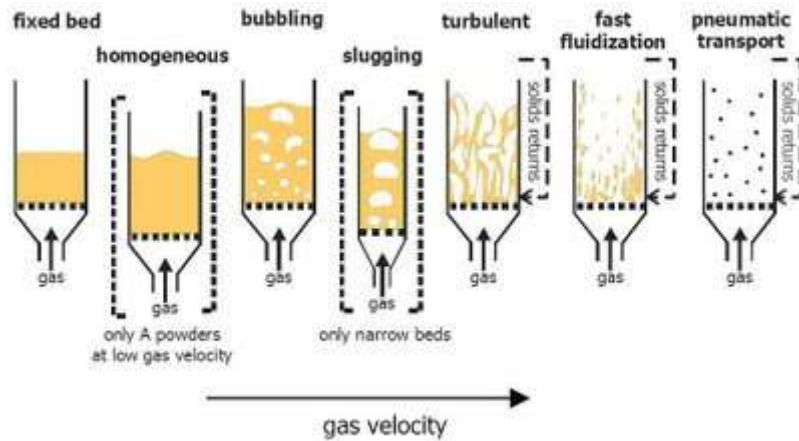


Figure 2-9: Fluidization regimes

When drag on the particles from a rising fluid stream exceeds the weight of the solids, the gravitational force exerted on the particles is overcome and the bed becomes fluidized. The minimum velocity at which the particles become suspended is known as the minimum fluidization velocity  $U_{mf}$ . Beyond this velocity, for a certain class of particles bubbles form immediately (Geldart Group B, D) whereas for other types of particle (Geldart Group A), bubbles form only when the velocity exceeds a minimum threshold called the minimum bubbling velocity  $U_{mb}$ . The point at which the gas velocity is sufficient to entrain particles entirely out of the bed is known at  $U_{tr}$  transport velocity – pneumatic transport. Many commercial processes operate in the turbulent fluidization regime for which the gas-solids contacting is greatest.

Equations 2-1 and 2-2 are used to find minimum fluidization velocity ( $U_{mf}$ ) (Kunii & Levenspiel, 1969).

$$Small\ Particles: \quad u_{mf} = \frac{d_p^2(\rho_s - \rho_g)g}{1650\mu} \quad Re_p < 20 \quad Eq.\ 2-1$$

$$Large\ Particles \quad u_{mf}^2 = \frac{d_p(\rho_s - \rho_g)g}{24.5 \rho_g} \quad Re_p > 1000 \quad Eq.\ 2-2$$

Experimentally the  $\Delta p$ -versus- $u_0$  diagram is particularly useful to determine the minimum fluidization velocity (Fig. 2-10)

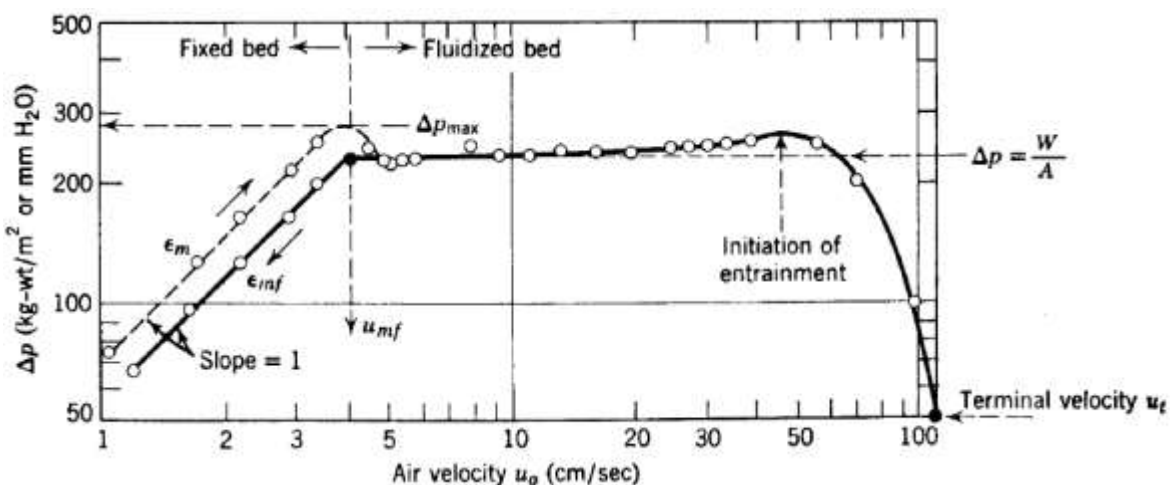


Figure 2-10: Typical diagram of pressure drop versus gas velocity (Kunii & Levenspiel, 1969)

Grouping of powders is based on density of particles and fluidization gas and particle size. The behavior of fluidized solids which have been divided into four groups (Geldart, 1973) (Fig. 2-11). The group C powder are fine particles in which fluidization is difficult, group A particles ranging from 20-200  $\mu\text{m}$  and fluidization starting above  $U_{mf}$ , in group B powders bubbling occurs when fluidization starts.

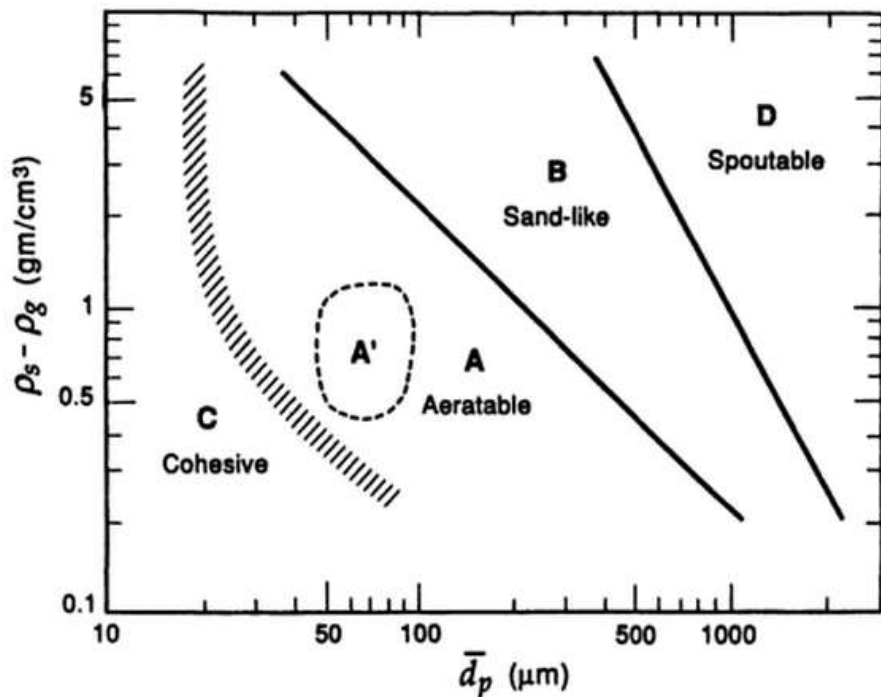


Figure 2-11: Geldart classification (Geldart, 1973)

## 2.6.2 Applications in industry

In 1941 fluidized beds were developed to crack oil to gasoline/diesel/jet fuel. Commercialization of this technology to other processes has been growing since (Table 2-2) for catalytic reactions, non-catalytic reactions, heat transfer, mass transfer like, acrylonitrile, Fischer-Tropsch synthesis, phthalic anhydride synthesis, methanol to gasoline and olefin, cracking of hydrocarbons (e.g. fluid catalytic cracking), coal combustion, coal gasification, cement clinker production, titanium dioxide production, calcination of  $\text{Al(OH)}_3$ , granulation drying of yeast, heat exchange, absorption and nuclear energy (uranium processing, nuclear fuel fabrication, reprocessing of fuel

and waste disposal) (Yang, 2003). The advantages of this type of reactor are; ease of solids handling, iso-thermal design options/flexibility and cost. Having extremely high heat transfer rates and the homogeneous distribution of reactants in the bed is most aspect to use this type of reactor. Some plants like; FCC regenerators, mobil MTG reactors, acrylonitrile, maleic anhydride, phthalic anhydride, ethylene dichloride and roasting of zinc sulfide use turbulent fluidized bed reactor (Bi, Ellis, Abba, & Grace, 2000).

Table 2-2: Commercial catalytic fluidized beds (Patience, G.S., 2013)

Product or Reaction	Process
Phthalic anhydride	Sherwin-Williams-Badger
Fisher-Tropsch Synthesis	Kellog, Sasol
Vinyl acetate	Nihon Gosei
Acrylonitrile	Sohio
Ethylene dichloride	BASF, ICI, Goodrich
Chloromethane	Asahi Chemical
Maleic anhydride	Mitsubishi, DuPont, Lonza
Polyethylene	Union Carbide
Polypropylene	Mitsui PetroChemical
O-cresol and 2,6-xylenol	Ashai Chemical

Using fluidized bed reactors to oxidize carbohydrate substrates in the presence of a metal catalyst and using a gas as oxidizing reagents has been disclosed in many studies in the laboratory and pilot plant (Anellotech – Huber, Zhang, et al., 2013) (Virent – (Kania et al., 2013)).

For oxidation, ammoxidation and carboxylation reactions between oxidizable reactant and oxygen in the presence of a solid catalyst in fluid bed reactor is suitable (Fiorentino, Newton, Salem, & Williams, 2003).

The selective oxidation of polysaccharides to produce polycarboxylic acids which uses nitrogen dioxide as oxidizing reagents and  $V_2O_5$  as catalyst, employs a fluidized-bed reactor (Engelskirchen, Fischer, Juettner, Moeller, & Verholt, 1998). Continuous oxidation of alditols to aldose using supported platinum, palladium, rhodium and ruthenium catalyst in the presence of oxygen is also carried out in a fluidized bed reactor (Arena, Blaise J & Schumacher, 1992).

## 2.7 Spray atomization

### 2.7.1 Mechanism of atomization

The classical study of how a falling stream of fluid breaks up into smaller drops has been studied by Rayleigh. Plateau (1873) found experimentally that a vertically falling water jet will break up into drops if its length is greater than about 3.13 to 3.18 times its diameter. Afterwards, Rayleigh showed theoretically that a vertically falling column of non-viscous liquid with a circular cross-section should break up into drops if its length exceeded its circumference (Strutt & Rayleigh, 1879).

Experimental observations beside nonlinear simulation of liquid jet breakup illustrated formation of a ligament between the main forming drops. This ligament rebounds and finally becomes spherical and forms the satellite drop (Vassallo & Ashgriz, 1991) (Fig. 2-12).



Figure 2-12: Stable satellite (Vassallo & Ashgriz, 1991)

Effervescent atomization creates small droplets. Adding of an inert gas will decrease the size of the droplet when the fluid exits the nozzle (Sovani, Sojka, & Lefebvre, 2001). It requires the addition of a pressurized gas to the liquid to be sprayed into droplets. The gas bubbles assist the disintegration of the liquid filaments. These filaments are then transformed into drops due to

capillary instability phenomena discussed above. Figure 2-13 shows the list of parameters affecting the size of the droplets in the atomization process of effervescent.

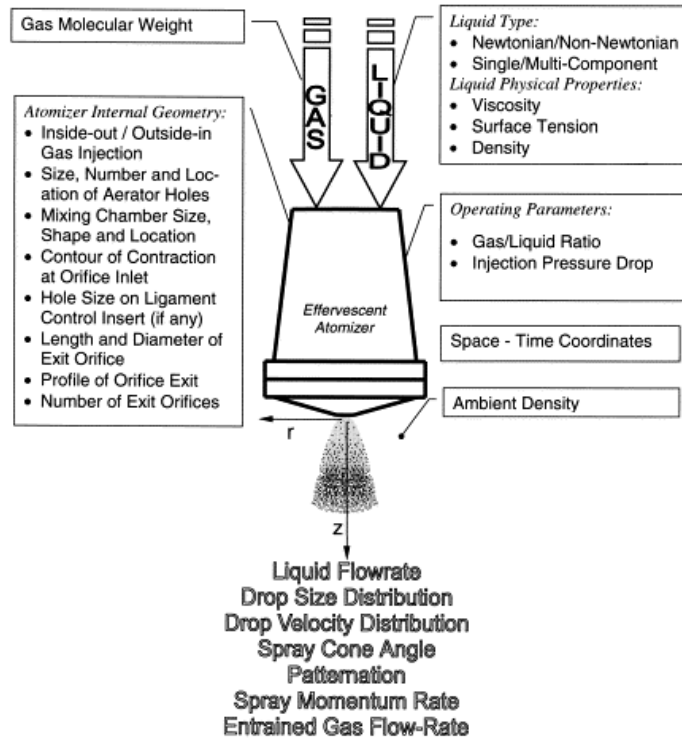


Figure 2-13: Variables in effervescent atomization (Sovani et al., 2001)

There are two types of two-fluid injectors, externally mixed and internally mixed. Internally mixed injectors are suitable for micro-fluidized bed since it needs less of co-fed gas (Fig. 2-14).

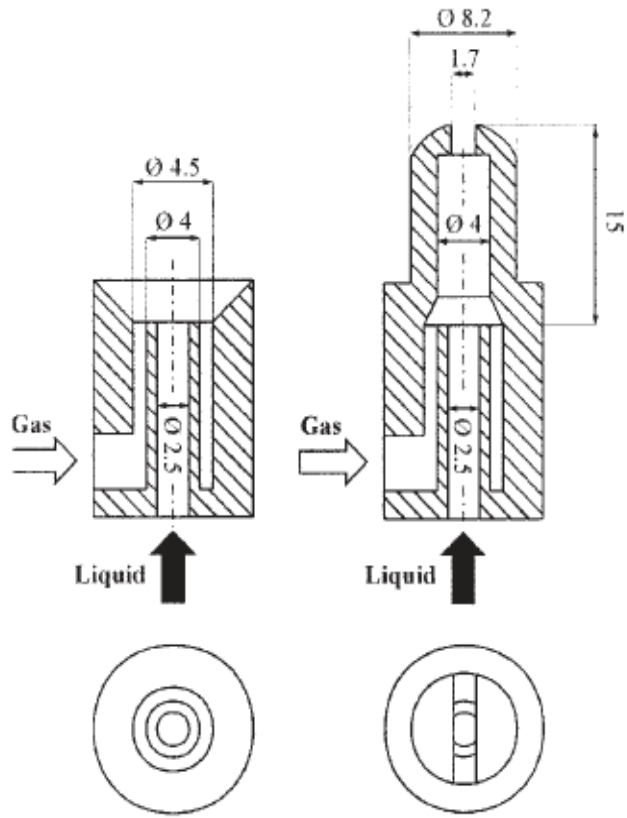


Figure 2-14: Two-fluid injectors; I) externally mixed, II) internally mixed

Electrospraying known as electro hydrodynamic atomization is a process in which a high electric field disperses a liquid that allows the formation of droplets. More specifically, the Coulomb electric forces will tend to oppose the surface tension then deform the jet and form droplets because of the electrical and mechanical forces. The scheme of the method is given in Figure 2-15. Figure 2-16 also shows this method with a circle shape ground electrode.

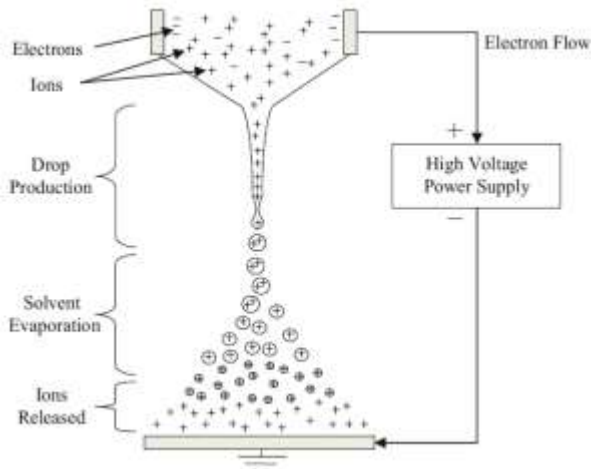


Figure 2-15: Electrospray mechanism (Sultan, Ashgriz, Guildenbecher, & Sojka, 2011)

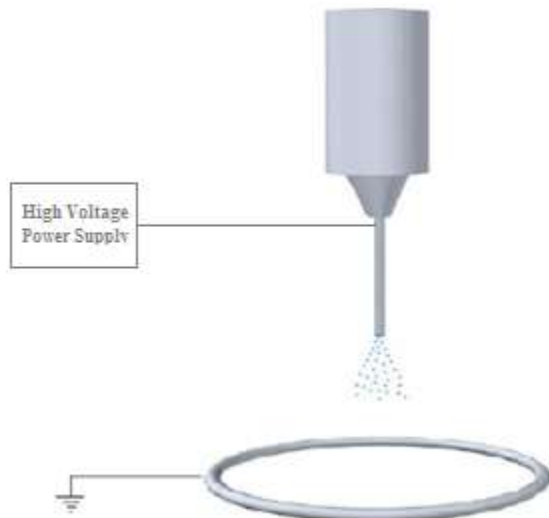


Figure 2-16: Schematic of electrospray with circle shape ground electrode

## 2.7.2 Applications in catalytic processes

The quality of the liquid injection has a significant impact on agglomerate formation and on product yield (Knapper, Gray, Chan, & Mikula, 2003). Good distribution of liquid feed and the droplet size of liquid feed sprayed into a fluidized bed reactor are very important. In a good atomization it will inject a gas and liquid through the bed of particles in specific conditions that

will react with the catalyst particle and transform to desired products. Parameters such as the temperature of the droplets as a function of the distance from the nozzle, particle-particle interaction (Bruhns & Werther, 2005), air-to-liquid ratio (ALR), the liquid mass flow rate, and the nozzle size (Portoghesi, Ferrante, Berruti, Briens, & Chan, 2008) have been studied.

The introduced liquid feed into catalyst bed of fluidized bed reactor wets the solid in the vicinity of injector. Agglomerated particles rise in the bed and mix. In the case of porous particles, agglomerates breakup easily but it slows down the drying rate (desorption) (Fig. 2-17).

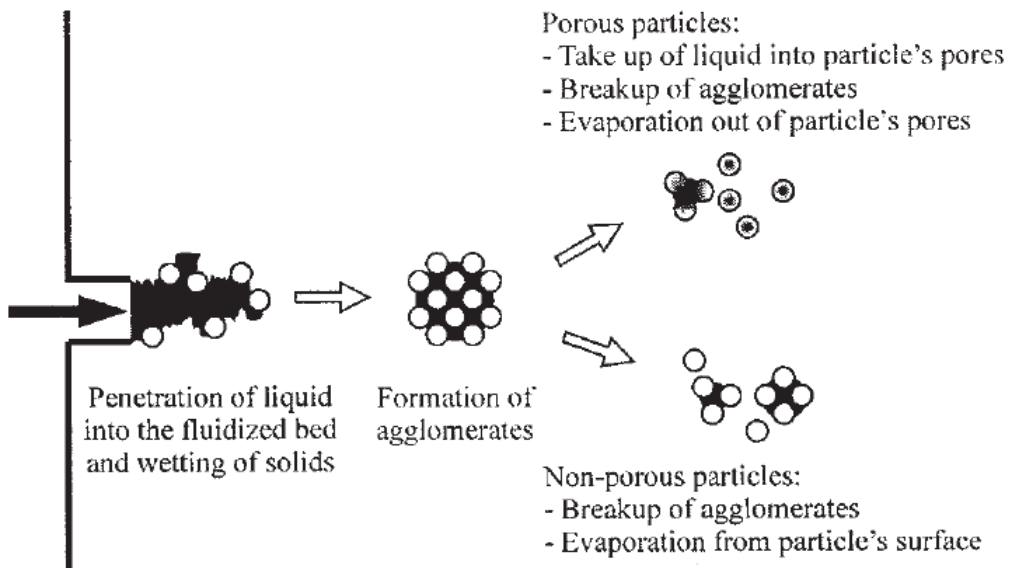


Figure 2-17: Particle characteristics critical - porous vs. non-porous particles (Bruhns & Werther, 2005)

Increasing the air/liquid ratio increases the spray efficiency. Smaller droplets form for higher Injected air/flow rate ratios increases the evaporation rate and heat transfer. It also increases the liquid/solid contact in the reactor and efficiency. Increasing the liquid flow rate and/or reducing the nozzle size improves atomization. On the other hand increasing nozzle size by keeping air and liquid flow constant, reduces the liquid-solid contact efficiency (Portoghesi et al., 2008).

## CHAPTER 3 ORGANIZATION OF THESIS

### 3.1 Original scientific hypotheses

**Hypotheses 1:** A fluidized bed reactor provides sufficiently high mass and heat transfer rates and minimizes of hot-spots near the reactant feed point by providing an efficient cooling by the latent heat of evaporation.

**Hypotheses 2:** Carbohydrates form organic carboxylic acids through heterogeneous catalysis and can provide a renewable feedstock for the chemical industry. For oxidation reactions, vanadyl pyrophosphate (VPP) was selected because of its strong acids cites and its commercial use in producing maleic anhydride from n-butane. Oxidation carried over vanadyl pyrophosphate (VPP) catalyst and other mixed metal oxide catalysts.

**Hypotheses 3:** Atomizing a liquid solution of xylose reduces its thermal decomposition and caramelization rate. Wet of solids agglomerates catalyst in the bed and at the nozzle tip. The atomized jet of liquid droplets and gas penetrate deep enough into the bed.

### 3.2 Methodology

First, a number of preliminary experiments have been conducted to prove the feasibility of the project. The aim of this project was to optimize the existing experimental configuration to inject a sugar solution in the fluidized bed while avoiding line blockage. These activities included improving the analytical capabilities, such as such as HPLC and GC, to identify and measure a whole range of targeted products. During these experiments, various catalyst candidates have been tested to identify the most promising and identify reaction pathways.

There were two separate phases in the project; phase I included commissioning a capillary fluidized bed reactor and feeding nozzle and operability experiments; purchasing and installing additional instrumentation such as HPLC and GC columns; calibrating suspected compounds; identification of unknown components. For commissioning, d-xylose was chosen as a representative carbohydrate due to its favourable cost compared to alternatives. In phase II, we identified and measured a range of targeted products b; completed a series of screening experiments to identify the most significant process parameters; optimized the operating

conditions based on an experimental design approach to maximize yields of the desired products. We also tested various catalysts.

### **3.3 Article**

To achieve the mentioned objectives, the thesis was conducted under the article entitled: “Partial oxidation of d-xylose to maleic anhydride and acrylic acid over vanadyl pyrophosphate” which is presented in chapter 4.

## **CHAPTER 4      ARTICLE 1 : PARTIAL OXIDATION OF D-XYLOSE TO MALEIC ANHYDRIDE AND ACRYLIC ACID OVER VANADYL PYROPHOSPHATE**

Touraj Ghaznavi, Cristian Neagoe, Gregory S. Patience

Department of Chemical Engineering, Polytechnique Montréal, C.P. 6079, Succ. CV Montréal,  
H3C 3A7 Québec, Canada

(Journal of Biomass and Bioenergy, DOI: 10.1016/j.biombioe.2014.09.029)

### **4.1 Presentation of the article**

This chapter introduces a new technology for the valorization of C5 sugars (xylose). We review current processes and the catalytic pathway using capillary fluidized bed reactor for the conversion of d-xylose to carboxylic acids. Products yield and other results are presented.

## 4.2 Abstract

Xylose is the second most abundant sugar after glucose. Despite its tremendous potential to serve as a renewable feedstock, few commercial processes exploit this resource. Here, we report a new technology in which a two fluid nozzle atomizes a xylose water solution into a capillary fluidized bed operating above 300 °C. Xylose-water droplets form at the tip of the injector, vapourize then react with a heterogeneous mixed oxide catalyst. A syringe pump metered a 3 %<sub>wt</sub> solution of xylose to the reactor charged with 1 g of catalyst. Product yield over vanadyl pyrophosphate was higher compared to molybdenum trioxide-cobalt oxide and iron molybdate; it reached 25 % for maleic anhydride (acid), 17 % for acrylic acid and 11 % for acrolein. The gas residence time was 0.2 s and after 4 h operation, the catalyst was free of coke – based on a thermogravimetric analysis of catalyst withdrawn from the reactor. Powder agglomerated at the tip of the injector at bed temperatures below 300 °C and with a 7 %<sub>wt</sub> xylose solution.

Keywords: xylose, vanadyl pyrophosphate, capillary fluidized bed, maleic anhydride, acrylic acid.

## 4.3 Introduction

Lignocellulosic biomass is the most abundant source of renewable green energy and consists of carbohydrate polymers (cellulose and hemicellulose) and aromatic polymers (lignin). Hard wood lignocellulose is approximately 40-50 % cellulose, 25-35 % hemicellulose and 20-25 % lignin [1]. Hemicellulose includes xylan, glucuronoxylan, arabinoxylan, glucomannan and xyloglucan. These soluble polysaccharides hydrolyse to form five carbon carbohydrates (simple sugar) among which d-xylose is the most abundant. Current technologies to process hemicellulose are limited to thermo-chemical to produce energy (in pulp mills) and biochemical (fermentation to ethanol). The latter process has attracted significant scientific attention to improve yeast strains as well as to formulate alternative process technologies – xylose to xylulose and then to ethanol, for example [2]. Target molecules for enzymatic processes (fermentation) include methanol, ethanol and butanol, which are principally used as a fuel [3]. However, fermentation is an inherently inefficient process in which the maximum carbon yields are relatively low [4]. The economics of these processes are improving with superior strains of enzymes [5].

Together with combustion, other thermo-chemical processes include gasification, pyrolysis and liquefaction that lead to methane, methanol, diesel, gasoline, olefins etc. [6, 7]. Catalytic fast pyrolysis of lignocellulosic biomass in a fluidized bed reactor over zeolite forms aromatic and olefinic hydrocarbons [8, 9]. Xylosan is formed by the pyrolysis of xylose, which is easily oxidized to give furfural and its acetylation yields diacetylxylosan [10]. These conventional bio-refinery approaches have a number of intermediate steps that impact negatively the profitability. Although thermo-chemical processes convert all the bio-mass, the high temperatures reduce the yield of desirable products and results in coke and other by-products.

Xylose dehydrates to furfural in the presences of acid catalysts, either Brønsted or Lewis [11]. Furfural was an intermediate to make THF (a solvent and a precursor of spandex fibres as well as adiponitrile), furfuryl alcohol, 2-methyltetrahydrofuran and furan [12-15]. In the presence of a base catalyst xylose can produce cyclic compounds [16]. Xylose is also hydrogenated to form xylitol, a sugar alcohol which is used as a humectant among other applications [17].

Currently, organic acids and anhydrides such as maleic, acrylic and methacrylic acid are produced by the partial oxidation of fossil based C3 to C4 alkanes and olefins. Maleic anhydride is a valuable monomer for unsaturated polyester resins, polyurethane, pharmaceuticals and agrochemicals. Annual acrylic acid production exceeds 4 000 t. Furfural and HMF oxidize to maleic acid and its isomers in the presence of a heterogeneous rhenium based catalyst, and a co-catalyst [18]. Glucose and lactose oxidize to gluconic acid and lactobionic acid using a gold catalyst [19]. Noble metal catalyst platinum or palladium, for example, oxidize monosaccharides to aldonic and gluconic acid under an alkaline condition [20]. Yields were highest with a palladium on carbon catalyst and oxygen. Xylose partially oxidizes to xylonic acid in the aqueous phase at low temperatures (25-60 °C) with gold, palladium or copper [21-23]. Xylonic acid and xylitol yields reach 80 % with electro technologies and xylose as a feedstock [24]. Other oxidation products of xylose include: trihydroxydiacid, aldaric acids (xylaric) [25, 26] and threonic acid, acetic acid and formic acid [27-29]. Electro-oxidation and metabolic processes have also been developed to produce xylonic acid glyceric, glycolic and formic acids [30] xylonate and xylonic acid [31-34].

Liquid-solids heterogeneous catalysis has been practiced for many years [20, 35]. Current work is dedicated to oxidation, hydrogenation or hydrolysis to organic acids and polyols. Activities are

ongoing to render these processes cost effective on a large scale. However, mass transfer limitations, low reaction rates and separating catalyst from the product are some of the common limitations. Gas phase-heterogeneous processes offer superior mass transfer, higher reaction rates while minimizing waste water and catalyst recycle issues. Moreover, they offer the potential to open up routes to producing other highly valued chemicals while reducing the number of process steps [36]. Fluid bed processes to oxidize carbohydrate streams in the presence of metal catalyst have reached the pilot plant stage [8, 37]. Engelskirchen et al. [38] disclosed a fluidized bed process in which nitrous oxidizes convert polysaccharides (starch) to polycarboxylic acid at temperatures below 160 °C.

In the process described herein, a xylose water solution is atomized directly into a fluidized bed operating at temperatures beyond 300 °C. The fluidized bed reactor combines the advantages of excellent gas-solids contacting and fast reaction kinetics associated with a thermo-chemical approach while minimizing the parasitic non-selective reactions since the temperature is several hundred degrees Celsius lower. Vaporizing carbohydrates starch, mono-saccharides, and polysaccharides can be difficult due to the kinetics of caramelization and the possibility of agglomerating catalyst: When heated, sugars decompose and may become cohesive.

The quality of the liquid spray has a significant impact on powder agglomeration, particularly at the nozzle tip [39]. Maintaining a fine spray to ensure the sparger tip remains clear was a challenge. Gas-assisted atomization minimizes the mean droplet, increases jet penetration and improves the liquid-solid contact efficiency. Parameters such as the temperature of the droplets as a function of the distance from the nozzle, particle-particle interactions [40], air-to-liquid ratio, the liquid mass flow rate, and the nozzle size have been evaluated [41]. Increasing the gas-to-liquid flow ratio and/or reducing the nozzle size increases the spray efficiency. In this study, we demonstrate the relationship between the experimental conditions and agglomeration at the tip. With respect to the catalyst, vanadyl pyrophosphate (VPP) is known to oxidize and dehydrate paraffins and olefins to maleic anhydride, furan, acetic, acrylic acids as well as methacrolein [42]. VPP is a multifunctional catalyst capable of isomerization, dehydrogenation, dehydration and oxidation reactions. We also tested, molybdenum trioxide-cobalt oxide and iron molybdate.

## 4.4 Experimental

### 4.4.1 Catalyst

Most experiments were conducted with commercial VPP supplied by DuPont [43]. In the first step of the catalyst synthesis, vanadium pentoxide was refluxed in a solution of isobutanol and benzyl alcohol and phosphoric acid for several hours forming vanadyl phosphate hemihydrate ( $\text{VOHPO}_4 \cdot \text{H}_2\text{O}$ ) crystals 70  $\mu\text{m}$  in diameter. After drying, the powder was air jet milled to 2 to 2.5  $\mu\text{m}$  then slurried together with polysilicic acid (~5 % silica and 45-50 % solids). The viscous slurry ( $\mu > 3000$  cP, depending on conditions) was pumped to the bottom of a 9 m diameter spray dryer and entered the vessel through a two fluid nozzle. During the drying process, silica migrated to the surface forming micro-spheres with a resistant shell – commonly referred to as the core-shell structure. The diameter of the powder ranged from 15  $\mu\text{m}$  to 200  $\mu\text{m}$  with a Sauter mean diameter of 70-80  $\mu\text{m}$ . It was calcined in the commercial regenerator for 5 hours at 3 atm and 390 °C and formed vanadyl pyrophosphate –  $(\text{VO})_2\text{P}_2\text{O}_7$  [44]. The partial pressure of water in the regenerator was less than 3 %<sub>vol</sub> and the oxygen concentration was greater than 15 %<sub>vol</sub>. The micro-spheres' surface was rough; many had smaller particles occluded to the surface that had formed during spray drying (Fig. 4-1). A fractured particle shows the internal porosity and complicated microstructure of the internal crystalline VPP. Energy-dispersive X-ray spectroscopy measurement confirmed that the powder was predominantly vanadium, phosphorous, silicon and oxygen with a small peak assigned to carbon (Fig. 4-2). The peaks in the XRD pattern correspond to those expected for the calcined vanadyl pyrophosphate phase before reaction with xylose, VPP (A), and after reaction, VPP (A<sub>ox</sub>). The pattern of the VPP (A<sub>ox</sub>) reflections is slightly sharper to crystal growth and crystallization of the amorphous VPP fraction (Fig. 4-3). The calcined VPP was gray to green in color. It had a particle density of 1700 kg m<sup>-3</sup> and a BET surface area of 34.9 m<sup>2</sup> g<sup>-1</sup> [45].

We also tested molybdenum trioxide/cobalt oxide (supplied by Arkema) and an iron molybdate catalyst –  $\text{Fe}_2(\text{MoO}_4)_3$  – which is used for methanol to formaldehyde process (prepared by Haldor Topsøe) [46, 47]. The  $\text{MoO}_3/\text{CoO}$  catalyst had the particle size of 60  $\mu\text{m}$ , BET surface area of 120 m<sup>2</sup> g<sup>-1</sup> and skeletal density of 3000 kg m<sup>-3</sup>. The iron molybdate catalyst was originally hollow

cylinders that we crushed and sieved the powder giving an average particle size of 125  $\mu\text{m}$ . It had a particle density of 800  $\text{kg m}^{-3}$  [48].

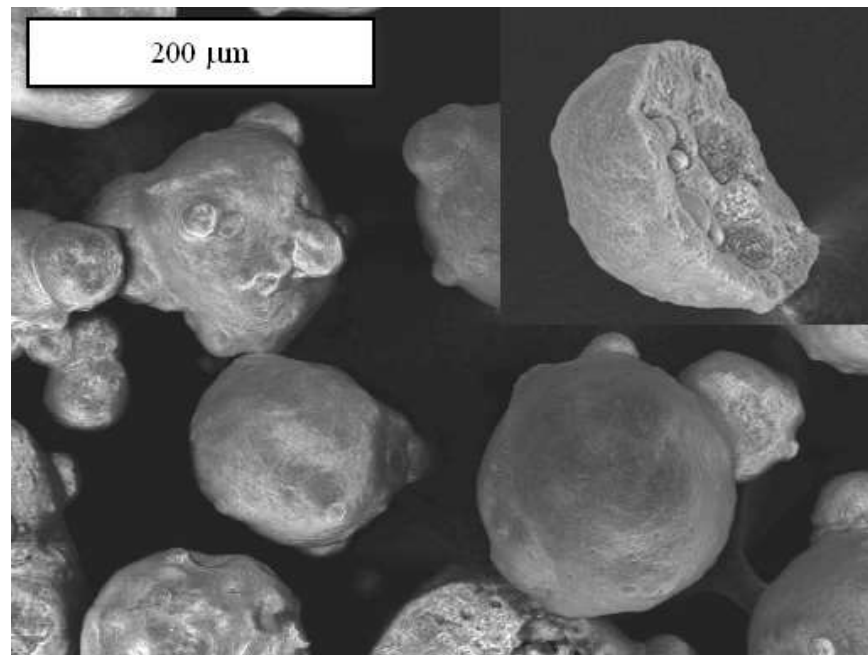


Figure 4-1: Calcined VPP SEM micrographs

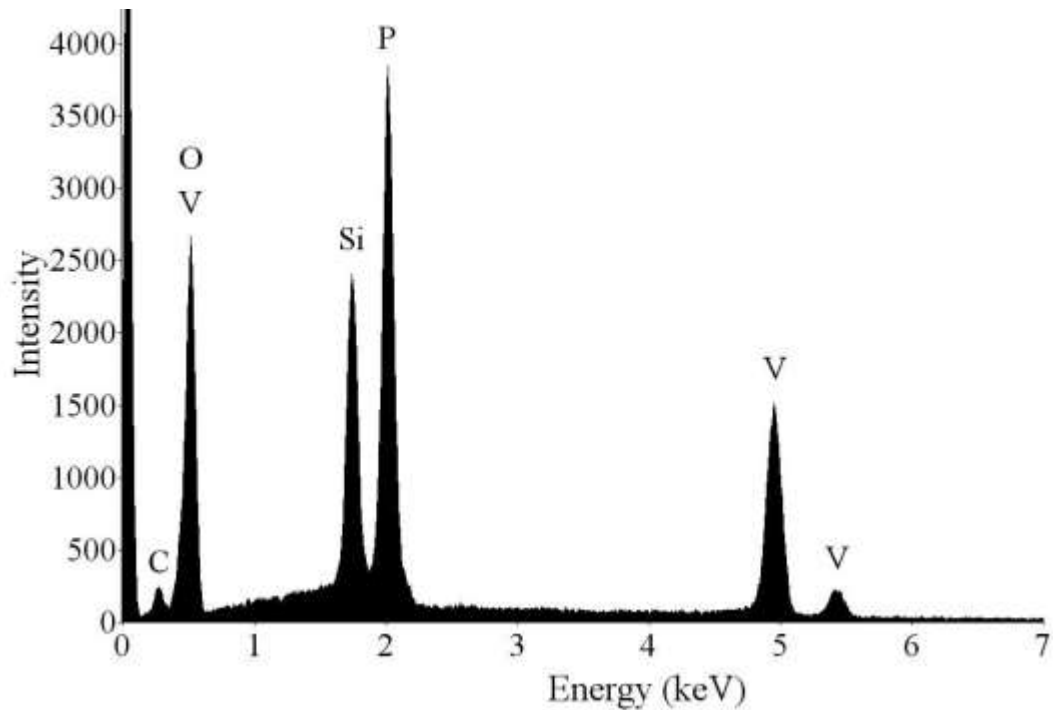


Figure 4-2: EDS trace of calcined VPP catalyst: carbon (C), oxygen (O), vanadium (V), silicon (Si)

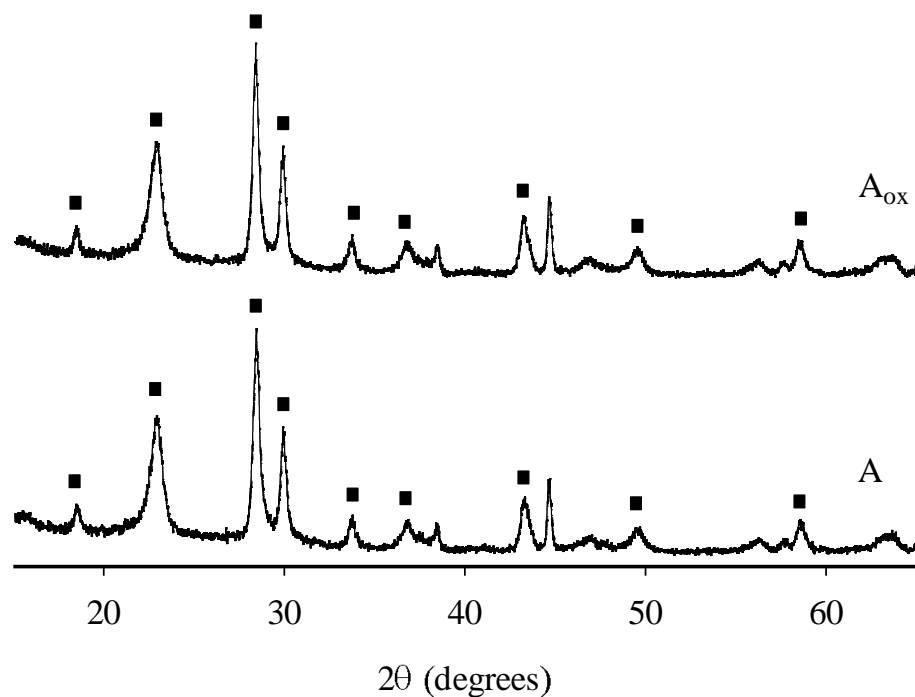


Figure 4-3: VPP XRD pattern: freshly calcined (A), after reaction (A<sub>ox</sub>), (■) (VO)<sub>2</sub>P<sub>2</sub>O<sub>7</sub>

#### 4.4.2 Capillary fluidized bed reactor

The quartz reactor tube was 700 mm long and 8 mm in diameter (ID) and was placed in a furnace that could operate at temperatures up to 1000 °C. A 3 mm thick fritted glass distributor positioned at 100 mm from the bottom such that the catalyst was in the bottom of the furnace (Fig. 4-4). With 1 g of catalyst ( $80 < dp < 180 \mu\text{m}$ ), the bed height was 30 mm. A sparger tube passed through a hole in the centre of the distributor and protruded in the bed by 8 mm. A syringe pump dosed the reactor at a rate of  $0.04 \text{ ml min}^{-1}$  with xylose-water solutions varying from 3 %<sub>wt</sub> to 7 %<sub>wt</sub>. Supplemental fluidization gas entered the reactor through the annulus of the distributor and contained from 0 to 21 %<sub>vol</sub> oxygen. Bronkhorst mass flow controllers (MFC) metered the gases going to the annulus and the sparger. A three point thermocouple entered the top of the reactor and extended down into the bed at 9 mm, 18 mm and 27 mm from the bottom of the bed to monitor the temperature along the bed axis. The thermocouple closest to the nozzle was always

lower than the two higher up in the bed: it was around 20 °C, 15 °C, 10 °C and 5 °C, for the experiments at 300 °C, 350 °C, 400 °C and 450 °C, respectively.

The operating window was established by varying temperatures from 200 °C to 550 °C, xylose solutions between 3 %<sub>wt</sub> and 7 %<sub>wt</sub>, fluidization gases with 0 %<sub>vol</sub> to 21 %<sub>vol</sub> oxygen (in nitrogen) and gas flow rates from 80-150 ml min<sup>-1</sup>. The operating window was selected from these scouting experiments for which product acid selectivity was highest from which an experimental design was established (Table 4-1). The reactor operated well within the range but agglomerates formed below 300 °C and with xylose concentrations above 3 %<sub>wt</sub> (Figs. 4-5 and 4-8). The gas contact time was 0.2 s and most experiments ran uninterrupted for 4 hours. The minimum fluidization velocity for VPP at ambient temperature was 0.5 cm/sec. We used four-way valves to dose the reactor with the air (for regeneration), nitrogen (for a purge) and the xylose solution. The nozzle was operated with gas-assisted atomization in which nitrogen was co-fed together with the xylose solution at 50 ml<sub>STP</sub> min<sup>-1</sup>. Scouting tests were made to identify optimal optimum spray conditions – defined as a uniformly distributed droplets formed in air at room temperature and pressure. The range of gas-to-liquid ratio was between 0.1-0.2 %<sub>wt</sub> with a solution flow rate of 0.01 to 0.1 ml min<sup>-1</sup> for a nozzle diameter of 0.25 mm and 0.5 mm. The lines blocked readily with capillary tubes less than 0.25 mm ID. The spray pattern looked best with a gas-to-liquid ratio fixed at 0.18 %<sub>wt</sub> and a liquid flow rate of 0.04 ml min<sup>-1</sup> with a 0.25 mm (ID) capillary tube constricted at the tip. The pressure at the injector gradually increased when the spray conditions were suboptimal indicating that the tip was beginning to block. Blockage was predominant at temperatures below 370 °C and in experiments with xylose concentrations exceeding 3 %<sub>wt</sub>. The injector pressure fluctuated between 0.5-0.7 bar at the beginning of the experiment and reached 2 bar after four hours of injection. Agglomeration was problematic when the pressure in the line reached approached 3 bar.

The reactor effluent passed through a series of quenches/bubblers to collect the liquid products (acids). A Varian ProStar HPLC equipped with a 325 type UV detector working at 210 nm measured the concentration of the product acids off-line. Compounds were separated with a MetaCarb 87H column (3007.8 mm) operating 60 °C. The liquid vector was a 0.02 N H<sub>2</sub>SO<sub>4</sub> solution flowing at 0.6 ml min<sup>-1</sup>. A Varian CP-3800 GC-FID confirmed the validity of the results. The GC had a DB-FFAP column (30 m × 0.320 mm × 0.25 μm). An Agilent 7890A GC-TCD with HayeSep and Molesieve 5Å columns quantified the non-condensable gas concentrations.

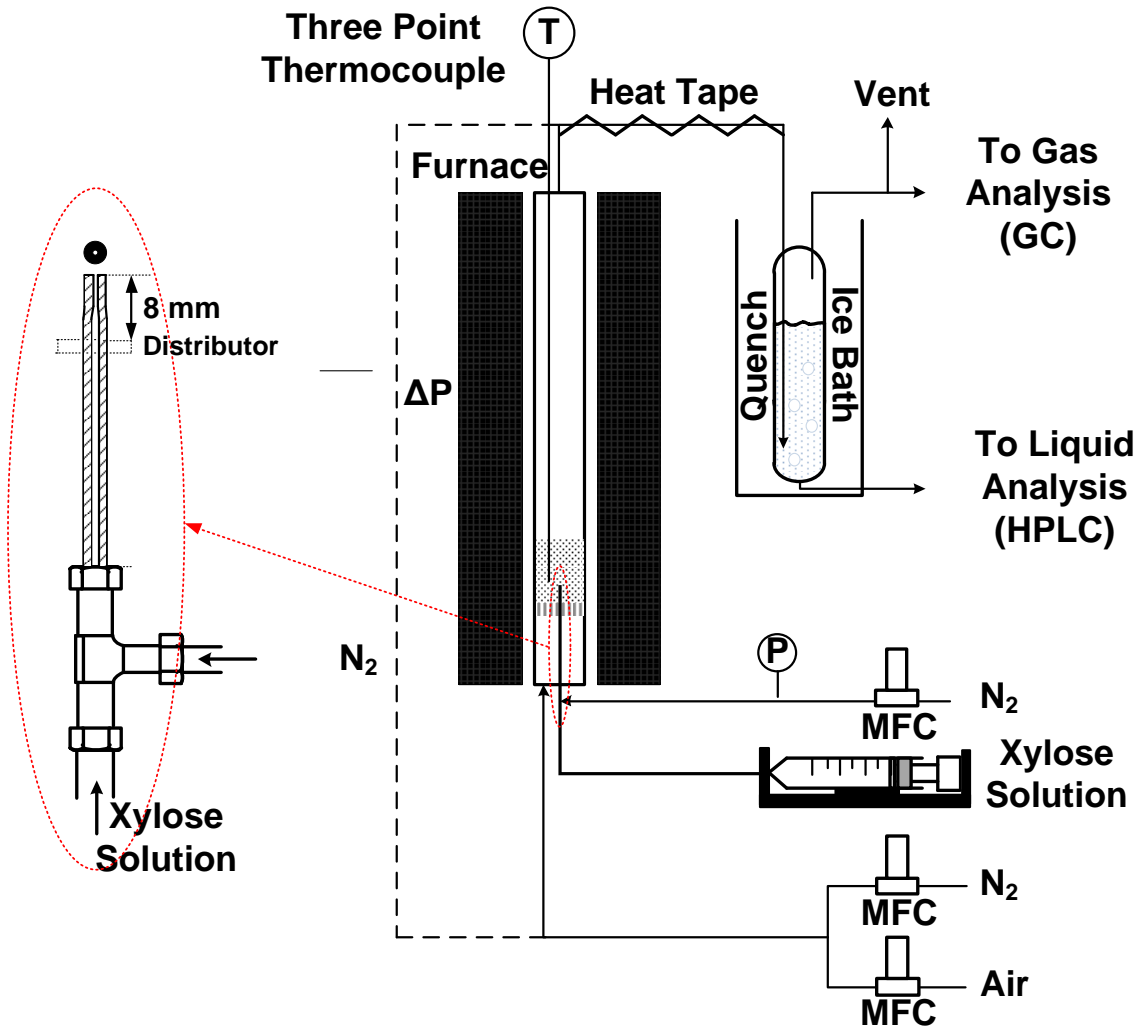


Figure 4-4: Experimental system schematic

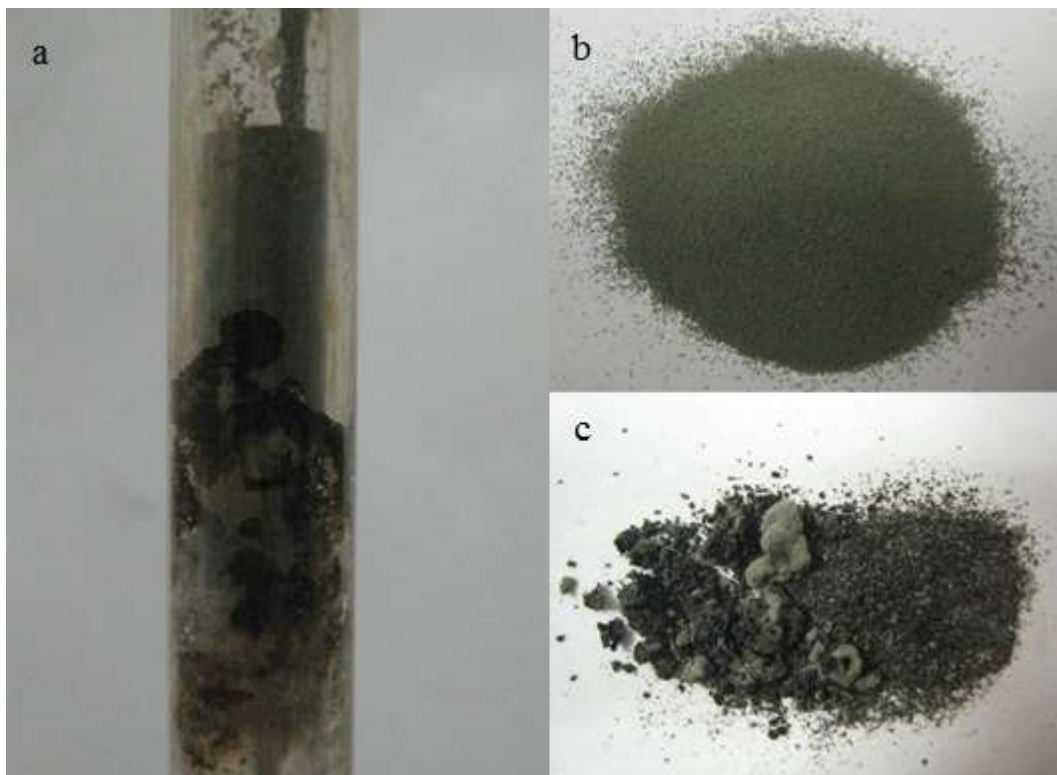


Figure 4-5: VPP powder morphology in tests conducted below 300 °C: (a) reactor tube, (b) 1-3 cm above the distributor, (c) 0-1 cm above the distributor

The selectivity was calculated as mole of each product divided by mole of fed xylose. The mass balance varied from 66.2 % to 98.1 % and was calculated based on the mass of carbon measured at the exit divided by the total carbon entering (D-xylose) (Eq. 1).

$$\text{Carbon Balance Closure (\%)} = \frac{\text{Carbon Out (g)}}{\text{Carbon In (g)}} \times 100 \% \quad (1)$$

Some of the D-xylose caused the catalyst to agglomerate while a small fraction formed carbon species on the catalyst, both of which contributed to the poor mass balance. The quantity of carbon on the catalyst was measured by thermogravimetric analysis.

## 4.5 Results and discussion

Product acid selectivity is sensitive to temperature, catalyst, space time and feed concentrations (O<sub>2</sub>, carbohydrate/sugar) and atomization performance. The major acids detected were maleic

acid and acrylic acid. However, we identified traces of methacrylic acid and possibly fumaric acid in the HPLC (Fig. 4-6).

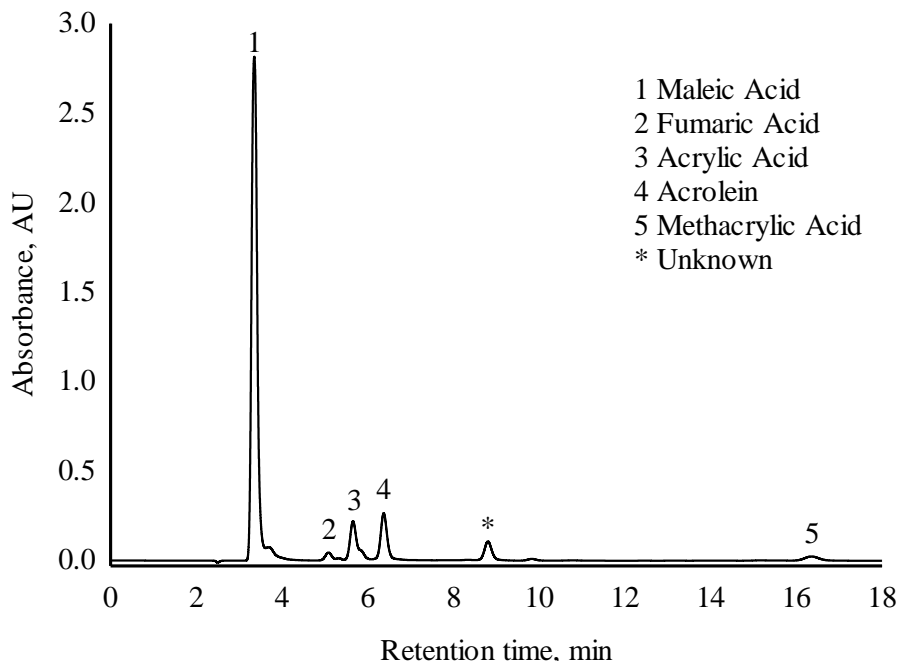
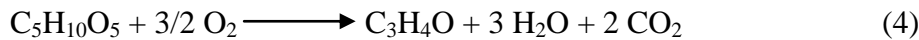
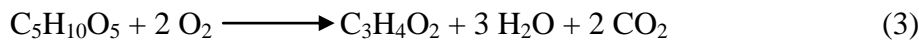
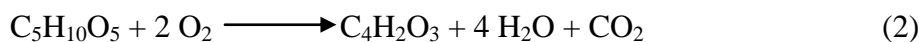


Figure 4-6: HPLC trace (3 %<sub>wt</sub> xylose, 350 °C and 3 %<sub>vol</sub> O<sub>2</sub>)

In blank experiments with silica sand at temperatures from 300 °C to 550 °C, we detected only carbon oxides. Xylose partial oxidation over VPP includes several reaction classes: C–C bond cleavage, C–O cleavage, and dehydration and forms maleic anhydride, acrylic acid and acrolein (Eqs. 2-4). It forms maleic anhydride, which subsequently hydrolyses to the maleic acid in the aqueous quench (Eq. 2). VPP is known to produce acrylic acid and acetic acid under oxygen deficient conditions [42] but the selectivity of acetic acid rarely exceeded 10 %, while the selectivity for acrylic acid was generally less than 2.5 %. It is unlikely that maleic anhydride is the precursor to acrylic acid (series reaction) but is formed through a parallel reaction pathway. Acrolein would be the most likely candidate as the intermediate for acrylic acid, but the change in concentration with conditions are very similar at all conditions.



The maleic anhydride selectivity approached 30 % at 350 °C and 10 %<sub>vol</sub> oxygen in the feed with VPP (Table 4-1). With 3 %<sub>vol</sub> oxygen in the feed, the maximum maleic anhydride selectivity (21 %) was recorded at 400 °C. Whereas the maleic anhydride showed local maximum while increasing temperature, both acrylic acid and acrolein decreased linearly from about 15 % at 300 °C to 5 % at 450 °C (Fig. 4-7).

Table 4-1: Product selectivity as a function of operation conditions

T °C	y <sub>O<sub>2</sub></sub> %	x <sub>XY</sub> %	Catalyst	Atomization Type	S <sub>MA</sub> %	S <sub>AA</sub> %	S <sub>Ac</sub> %	S <sub>CO<sub>2</sub></sub> %
300	3	3	VPP	a	15.0	11.2	13.7	41.0
300	3	7	VPP	a <sup>†‡</sup>	6.5	11.0	6.5	45.4
300	3	3	MoO <sub>3</sub> /CoO	a <sup>†</sup>	2.4	3.4	6.6	52.4
300	3	3	FeMoO	a	1.8	3.0	2.0	64.9
300	3	3	VPP	a <sup>†‡‡</sup>	13.3	5.6	5.0	-
300	3	3	VPP	b <sup>†‡</sup>	14.2	7.4	8.8	52.0
300	10	3	VPP	a	25.3	16.7	10.5	47
300	10	3	VPP	a <sup>†*</sup>	19.2	9.4	7.0	-
350	3	3	VPP	a	18.4	9.0	8.0	46.3
350	3	3	VPP	b <sup>†‡</sup>	15.9	6.7	6.6	57.0
350	10	3	VPP	a	27.5	7.6	8.8	51.1
400	3	3	VPP	a	21.0	7.4	6.6	50.4
400	3	3	VPP	b <sup>†‡</sup>	17.7	6.3	5.3	53.4
400	3	3	VPP <sup>†</sup>	a	21.4	7.8	7.2	40.7
400	10	3	VPP	a	21.2	7.8	6.2	57.5
400	10	3	VPP <sup>†</sup>	a	21.7	8.0	6.4	55.0
450	3	3	VPP	a	9.1	4.7	5.4	53.6
450	3	3	VPP	b <sup>†‡</sup>	3.9	1.0	4.3	59.0
450	10	3	VPP	a	11.4	2.9	5.8	63.8

Conversion (X=100 %), Xylose mass fraction (x<sub>XY</sub>), Oxygen volume fraction (y<sub>O<sub>2</sub></sub>), Selectivity (S), Maleic Acid (MA), Acrylic Acid (AA), Acrolein (Ac), Agglomeration (†), Blockage (\*), Sequential injection (†) (otherwise, continuous injection), Two hour experiment (†) (otherwise, four hour experiment)

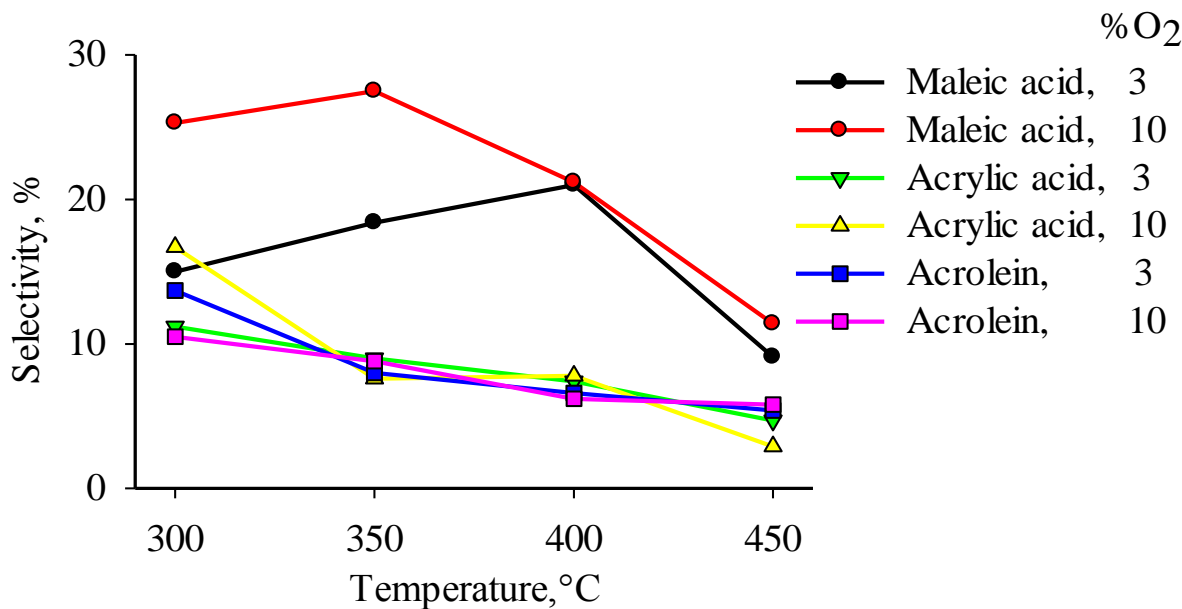


Figure 4-7: Product yield as a function of temperature and oxygen

Yields of maleic acid are higher with 10 %<sub>vol</sub> oxygen in the feed versus 3 %<sub>vol</sub> but for acrylic acid and acrolein, the differences are less pronounced: The yield was highest with 10 %<sub>vol</sub> oxygen at 300 °C and it was the lowest with the same oxygen at 450 °C. Acrolein was much less sensitive to temperature; furthermore, it was independent of the oxygen partial pressure.

Catalyst productivity was constant during the four hour in which the xylose was fed to the reactor: Yield remained the same after two hour continuous operation and four hours (Table 4-1). Further long term stability studies of 100 h on-stream operation would be necessary to conclude that deactivation is not an issue, but these preliminary tests are encouraging. It demonstrates that caramelization is minimal otherwise we would have expected some change in catalyst performance as xylose (or coke) accumulated on the catalyst surface.

Increasing the xylose weight percentage, however, was problematic. During the scouting experiments, we injected xylose concentrations greater than 3 %<sub>wt</sub> and in these tests catalyst agglomerated at the tip of the nozzle soon after the pump was initiated. In some cases the agglomeration was so severe that the quartz capillary tube broke (Fig. 4-8).



Figure 4-8: VPP agglomeration with 7 %<sub>wt</sub> xylose

Both  $\text{MoO}_3/\text{CoO}$  and  $\text{FeMoO}$  catalyst were tested. Although the desired acid yields were lower compared to VPP (Table 1) other compounds were detected by HPLC. At the end of the 4 h period the  $\text{MoO}_3/\text{CoO}$  agglomerated (Fig. 4-9) while the iron molybdate remained as a free flowing powder.

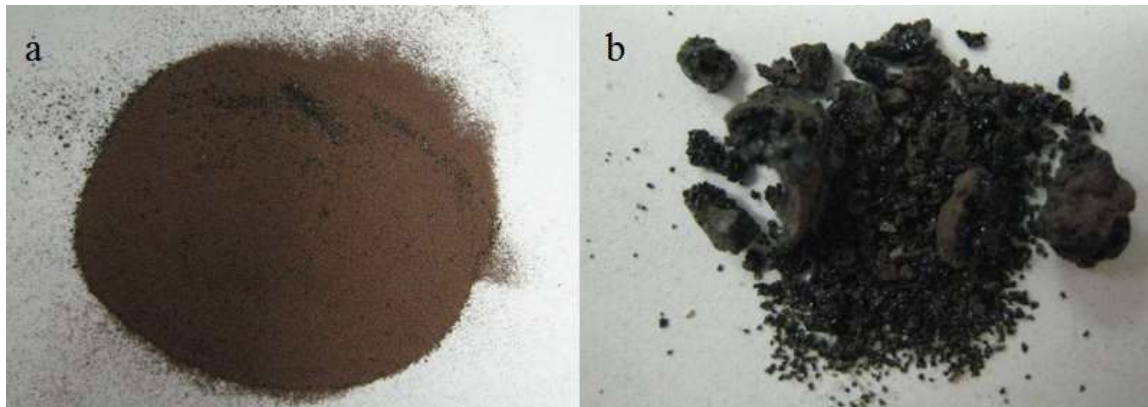


Figure 4-9:  $\text{MoO}_3/\text{CoO}$  powder morphology in tests conducted at 300 °C: (a) 1-3 cm above the distributor (second zone), (b) 0-1 cm above the distributor (first zone)

#### 4.5.1 Atomization

Atomizing suspensions through nozzles in spray dryers is a fundamental unit operation to produce powders. Atomizing liquids into fluidized bed is also practiced commercially for several catalytic processes including cracking of petroleum, fluid coking to upgrade bitumen and propylene polymerization where propylene is injected as a liquid. In fluidized beds, powders may agglomerate due to poor mixing between the gas and solids, insufficient velocity at the nozzle and poor heat transfer between the phases. For example, Darabi et al [49] report that agglomeration tendency in fluid cokers is lower at temperatures below 400 °C than at 500 °C. Bruhns and Werther [40] injected ethanol and water into bubbling fluidized beds operating at 120 to 160 °C. Agglomerates formed at the nozzle and broke up in the bed as the fluid evaporated. In DuPont's commercial butane oxidation [43] agglomerates as large as footballs collected in the cone region of the regenerator and stripper and at the bottom of the transport bed. These massive clumps could weigh 5 kg. They may have formed continuously during the process and

accumulated in stagnant regions. However, they were also thought to form during emergency shut downs when in which there was insufficient time to purge the reaction gases that could contain up to 10 %<sub>vol</sub> or more water vapour.

VPP agglomerates formed least when the xylose solution was atomized into small uniform droplets at the nozzle tip. We categorize the spray performance into four types designated as 'a', 'b', 'c', and 'd' (Fig. 4-10) depend on gas to liquid mass ratio which have been captured in ambient and their effect on VPP catalyst at the end of operation designated as 'a', 'b', 'c' and 'd'. The gas to liquid ratio was 0.18 %<sub>wt</sub> for Type 'a', 0.16 %<sub>wt</sub> for Type 'b', 0.14 %<sub>wt</sub> for Type 'c', and 0.12 %<sub>wt</sub> for Type 'd'. Type 'a' atomization disperses the droplets best and most uniformly – agglomeration at the tip was minimal. Type 'b' atomization was quite good in the central axis but ligaments or strands formed between the main drops. These strands would coalesce into satellite drops and this coalescence may have increased the build up of powder around the sparger tip. A fraction of the type "c" is well dispersed otherwise it produces larger droplets and, consequently, more agglomeration at the sparger tip. Type "d" is poorly atomized with liquid jets forming big drops throughout the cone of the spray.

The product yield was best when a fine spray formed at the nozzle tip (Fig. 4-11). Yield of maleic anhydride was approximately 5 %<sub>abs</sub> lower with the Type 'a' atomization compared to the Type 'b' atomization. At 450 °C, virtually acrylic acid production was virtually zero with Type 'b' atomization whereas its yield was around 5 % with Type 'a'. The acrolein yield was substantially higher with Type 'a' atomization at 300 °C. In fact, for all compounds, the trends for both types of atomization were the same, only the yields were lower for Type 'b' atomization.

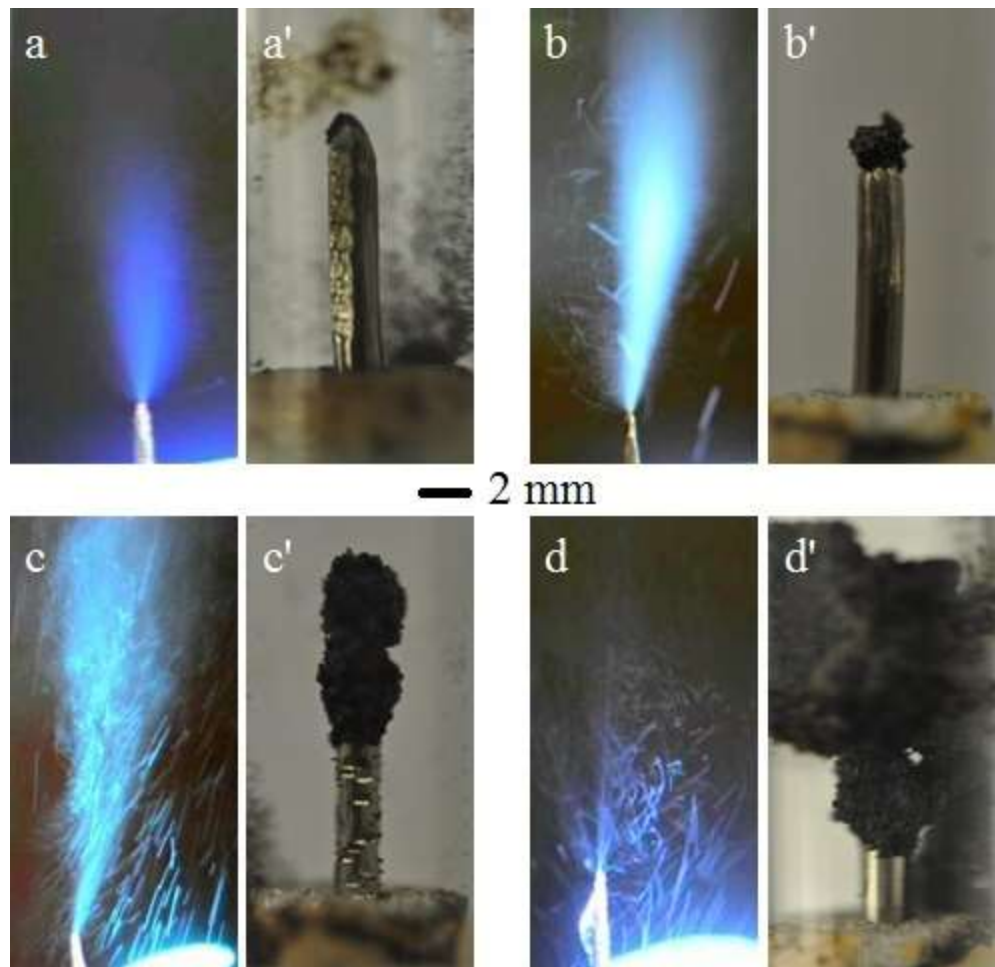


Figure 4-10: Atomization types in ambient (a, b, c and d) and their effect on VPP catalyst agglomeration at the nozzle tip (a', b', c' and d')

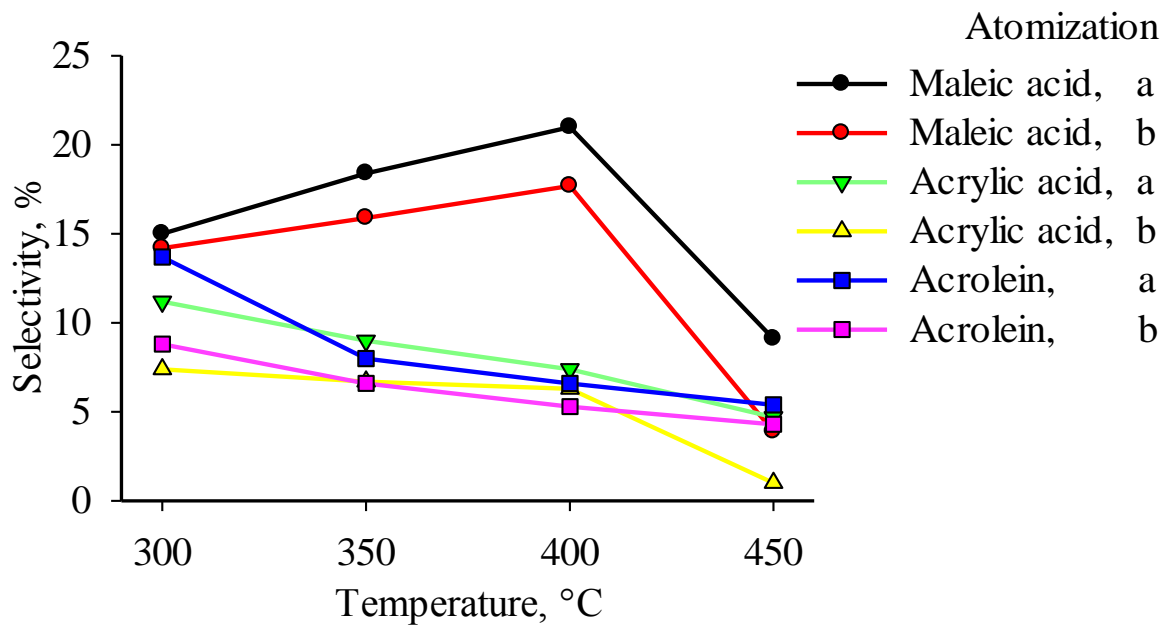


Figure 4-11: Effect of atomization on product yield for experiments with 3 %<sub>vol</sub> O<sub>2</sub> with VPP catalyst

We also tested a cyclic liquid injection followed by gas phase oxidation sequence. Switching between the liquid phase and gas phase injection was problematic. Flow regimes change when the injector is started and stopped. Under steady (optimized) conditions, the spray is fine and uniform (Fig. 4-10a) and the sparger tip remains practically clear. When the flow rate of gas is reduced (or the liquid injection rate increased), larger droplets appear and uniformity decreases (Fig. 4-10b). As a result, agglomerates begin to form at the sparger tip (but the bed remains fluidized). Columns of agglomerates form at the tip when the droplets are larger. When the sequence between liquid injection and gas phase oxidation is less than five minutes, the nozzle tips blocks during the four hour experiment. The nozzle blocked in less than 30 min for a frequency of one and three minutes. The forced concentration cycling was a means we anticipated that could be useful to regenerate catalyst that became coked or caramelized. However, more work is required to define the procedure in order to avoid blockage of the sparger tip when cycling between liquid injection and gas phase oxidation.

#### 4.5.2 Coke formation

To test the tendency for xylose to coke the catalyst, 25 mg samples of VPP were withdrawn from the reactor at the end of the experiments carried out with Type 'a' atomization (3 %<sub>wt</sub> xylose) and placed in a thermogravimetric analyzer (TGA/SDTA851<sup>e</sup> Mettler Toledo). The temperature ramp was set at 5 °C min<sup>-1</sup> and the final temperature was 550 °C. In one series of experiments, air was fed to the TGA at 20 ml min<sup>-1</sup> (Fig. 4-12) and in a second series, nitrogen was fed to the TGA at the same volumetric flow rate (Fig. 4-13). In the series with nitrogen, after the temperature reached 550 °C air substituted the nitrogen and the temperature was maintained for an additional 30 min. In all TGA tests, the weight loss was higher for the conditions in which the catalyst was operated at a lower oxygen concentration. Furthermore, the weight loss was generally lower for the tests conducted at higher temperature: The weight loss of the tests run at 400 °C was less than 2 % whereas it was as high as 5 % for the experiments at 300 °C. When the gas feed was switched from nitrogen to air, the mass increased by 0.7 % irrespective of the conditions. This mass gain is presumably due to the oxidation of V<sup>4+</sup> to V<sup>5+</sup> (from (VO)<sub>2</sub>P<sub>2</sub>O<sub>7</sub> to 2VOPO<sub>4</sub>). Most of the curves drop gradually to a constant weight with either nitrogen or as the feed gas. However, there is an additional weight loss at around 350 °C for xylose experiments run at 300 °C and 350 °C with 10 %<sub>vol</sub> in the feed.

Presumably, since the forms of the TGA curves and the weight loss remains essentially the same with nitrogen or air in the feed gas, we could conclude that the carbon accumulation is due to poorly volatile compounds – xylose, intermediates and maybe water – but not necessarily coke. We consider 5 %<sub>wt</sub> build up on the catalyst reasonably low compared to other processes. In fluid catalytic cracking, coke forms on the within ten seconds; for methanol-to-olefins with a SAPO catalyst, activity loss is significant after 10 minutes, with ZSM-5, the process can operate several hours; coke build up for the process to dehydrate glycerol takes as much as 24 h. Regardless of the form of the compounds on the VPP, a periodic regeneration step might be required to maintain catalytic activity.

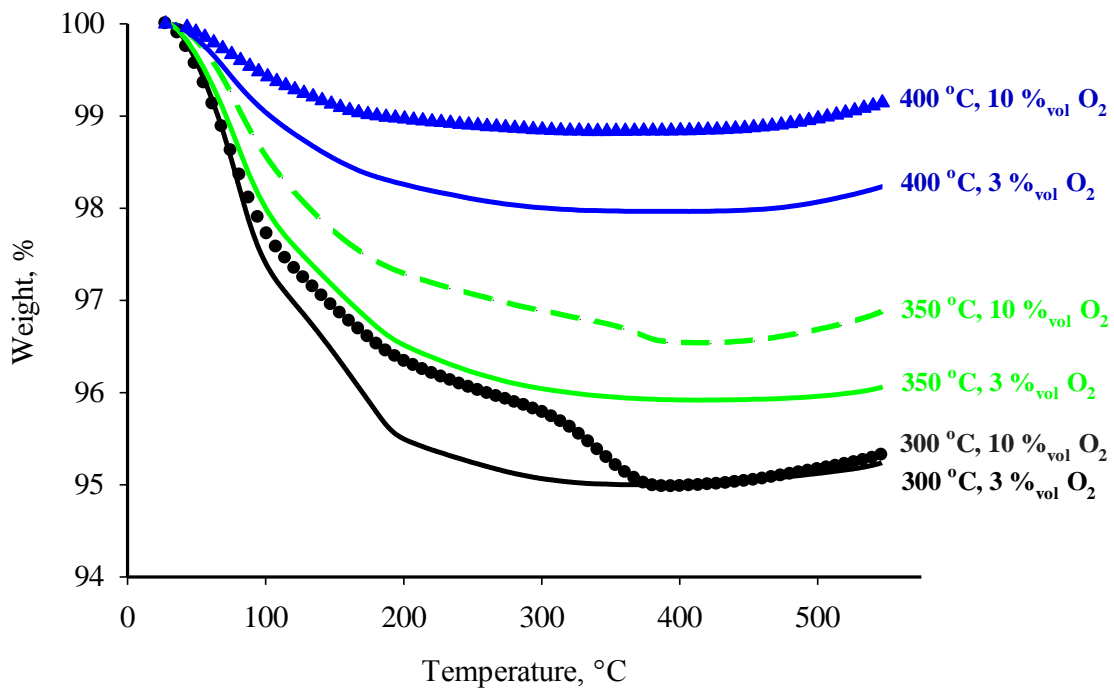
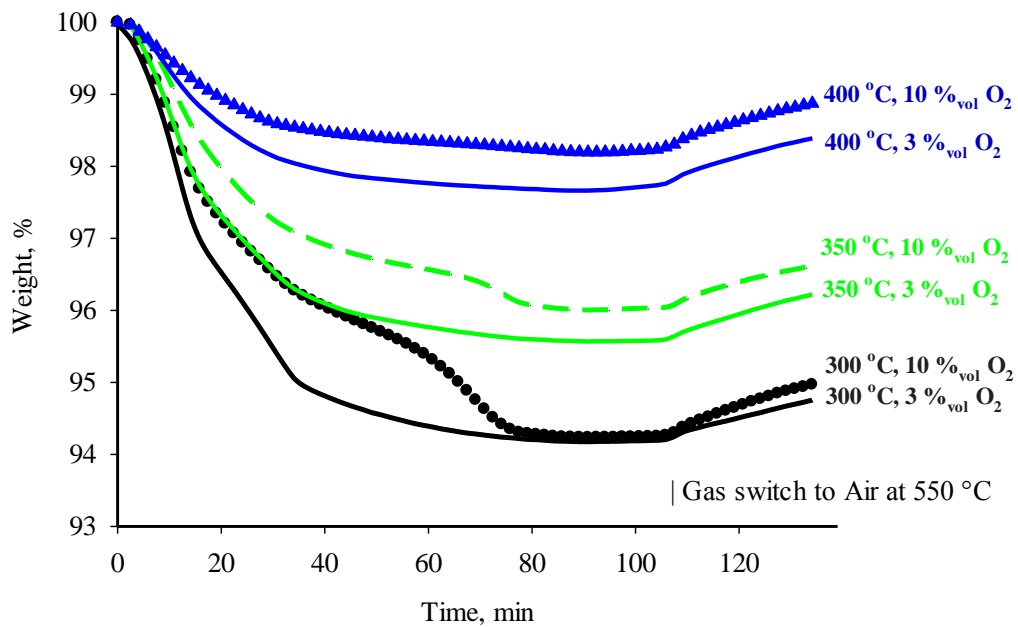


Figure 4-12: VPP TGA with air

Figure 4-13: VPP TGA with N<sub>2</sub>

## 4.6 Conclusions

Xylose reacts to form value added chemicals in the gas phase at temperatures beyond 300 °C. Gas-solids fluidized bed are ideal contactors for this reaction because of the high heat and mass transfer rates ( $> 700 \text{ W m}^{-2} \text{ K}^{-1}$ ) that ensure the xylose evaporates and reacts catalytically before it caramelizes. Conversion of xylose was 100 % of which almost 50 % was maleic anhydride (the most abundant compound), acrylic acid and acrolein. The optimum temperature was 350 °C and higher oxygen concentrations favored maleic anhydride yield whereas acrylic acid and acrolein were most sensitive to temperature: their highest yield was at 300 °C. TGA tests confirm that VPP gains as little as 2 %<sub>wt</sub> after 4 h continuous operation at 400 °C but that it gains up to 5 %<sub>wt</sub> at 300 °C. This weight gain is easily removed with a regeneration step and is considered low compared to other processes. Atomizing the xylose and increasing its feed concentration are two factors that require further work for scale-up.

## 4.7 Acknowledgments

The authors acknowledge E. I. du Pont de Nemours and Company (DuPont) for supplying the VPP and financial support from the Natural Sciences and Engineering Research Council of Canada (NSERC).

## 4.8 References

- [1] D. Fengel, D. Grosser, Holz Roh. Werkst. 33 (1975) 32-34.
- [2] A. Lachke, Resonance 7 (2002) 50-58.
- [3] A. Singh, P. Mishra, Microbial pentose utilization: current applications in biotechnology, Elsevier, Amsterdam, (1995).
- [4] M.E. Himmel, T. Vinzant, S. Bower, J. Jechura, BSCL use plan: solving biomass recalcitrance, National Renewable Energy Laboratory, NREL/TP-510-37902, (2005).
- [5] C. Beatty, S. Potochnik, G. Pease, US 20090275098 A1 (2009).
- [6] J.R. Regalbuto, Green Gasoline at NSF, ACS Green Chemistry and Engineering Conference, Jun 25 (2009), University Park, MD.

- [7] E.L. Kunkes, D.A. Simonetti, R.M. West, J.C. Serrano-Ruiz, C.A. Gärtner, J.A. Dumesic, *Science* 322 (2008) 417-421.
- [8] G.W. Huber, H. Zhang, T. Carlson, US Patent 20130060070 A1 (2013).
- [9] G.W. Huber, Y.T. Cheng, Z. Wang, W. Fan, US Patent 20130324772 A1 (2013).
- [10] C.D. Hurd, L.L. Isenhour, *J. Am. Chem. Soc.* 54 (1932) 693-698.
- [11] A. Fuente-Hernández, P.O. Corcos, R. Beauchet, J.M. Lavoie, *Biofuels and Co-Products Out of Hemicelluloses, Liquid, Gaseous and Solid Biofuels - Conversion Techniques* (2013).
- [12] J.G. Stevens, R.A. Bourne, M.V. Twigg, M. Poliakoff, *Angew. Chem.* 122 (2010) 9040-9043.
- [13] T. Wabnitz, D. Breuninger, J. Heimann, R. Backes, R. Pinkos, US 20100099895 A1 (2010).
- [14] T. Wabnitz, D. Breuninger, J. Heimann, R. Backes, R. Pinkos, US 8168807 B2 (2012).
- [15] W. Zhang, Y. Zhu, S. Niu, Y. Li, *J. Mol. Catal. A-Chem.* 335 (2011) 71-81.
- [16] T. Popoff, O. Theander, *Carbohyd. Res.* 48 (1976) 13-21.
- [17] J. Wisniak, M. Hershkowitz, R. Leibowitz, S. Stein, *Ind. Eng. Chem. Prod. RD.* 13 (1974) 75-79.
- [18] R. Saladino, A. Farina, US Patent 8609895 B2 (2013).
- [19] D.T. Thompson, *Top. Catal.* 38 (2006) 231-240.
- [20] K. Hattori, M. Ishii, M. Matsuda, B. Miya, H. Saito, H. Takizawa, H. Watanabe, US 4108891A (1978).
- [21] W. Bonrath, J. Fischesser, US Patent 20100217017 A1 (2010).
- [22] U. Prüße, K. Heidkamp, N. Decker, M. Herrmann, K.D. Vorlop, *Chem-Ing-Tech.* 82 (2010) 1231-1237.
- [23] R. Van der Weijden, J. Mahabir, A. Abbadi, M. Reuter, *Hydrometallurgy* 64 (2002) 131-146.
- [24] A. Jokic, N. Ristic, M. Jaksic, M. Spasojevic, N. Krstajic, *J. Appl. Electrochem.* 21 (1991) 321-326.
- [25] D.E. Kiely, K.R. Hash, US Patent 20080033205 A1 (2008).
- [26] F.R. Venema, J.A. Peters, H. van Bekkum, *J. Mol. Catal.* 77 (1992) 75-85.
- [27] H.S. Isbell, H.L. Frush, E.T. Martin, *Carbohyd. Res.* 26 (1973) 287-295.
- [28] E.O. Odebunmi, A.S. Ogunlaja, S.O. Owalude, *J. Chil. Chem. Soc.* 55 (2010) 293-297.
- [29] A.K. Singh, S. Srivastava, J. Srivastava, R. Singh, *Carbohyd. Res.* 342 (2007) 1078-1090.
- [30] A. Governo, L. Proenca, P. Parpot, M. Lopes, I. Fonseca, *Electrochim. Acta* 49 (2004) 1535-1545.
- [31] K. BERNHAUER, E. Riedl-Tumova, *Biochem. Z.* 321 (1949) 26-30.
- [32] J. Buchert, L. Viikari, M. Linko, P. Markkanen, *Biotechnol. lett.* 8 (1986) 541-546.

- [33] A. Hayasida, Biochem. Z. 298 (1938) 169-178.
- [34] H. Ishizaki, T. Ihara, Y. J. S. M, T. Imai, J. Agr. Chem. Soc. Jpn. 47 (1973) 755-761.
- [35] J.N. Chheda, G.W. Huber, J.A. Dumesic, Angew. Chem. Int. Edit. 46 (2007) 7164-7183.
- [36] M. Oh-Kita, T. Kita, EP0168826 B1 (1988).
- [37] J. Kania, P. Blommel, E. Woods, B. Dally, W. Lyman, R. Cortright, US 20130263498 A1 (2013).
- [38] K. Engelskirchen, H. Fischer, W. Juettner, T. Moeller, H.-W. Verholt, US 5821360 A (1998).
- [39] B.A. Knapper, M.R. Gray, E.W. Chan, R. Mikula, Int. J. Chem. React. Eng. 1 (2003).
- [40] S. Bruhns, J. Werther, AIChE J. 51 (2005) 766-775.
- [41] F. Portoghesi, L. Ferrante, F. Berruti, C. Briens, E. Chan, Powder Technol. 184 (2008) 1-10.
- [42] M.J. Lorences, G.S. Patience, F.V. Díez, J. Coca, Ind. Eng. Chem. Res. 42 (2003) 6730-6742.
- [43] G.S. Patience, E. Bordes-Richard, Appl. Catal. A 376 (2010) 1-3.
- [44] G.S. Patience, R.E. Bockrath, J.D. Sullivan, H.S. Horowitz, Ind. Eng. Chem. Res. 46 (2007) 4374-4381.
- [45] A. Shekari, G.S. Patience, Catal. Today 157 (2010) 334-338.
- [46] H.F. Rase, Oxidation, Handbook of Commercial Catalysts: Heterogeneous Catalysts, CRC press2000, pp. 282-287.
- [47] A.P.V. Soares, M.F. Portela, A. Kiennemann, Cataly. Rev. 47 (2005) 125-174.
- [48] A. Godefroy, G.S. Patience, R. Cenni, J.-L. Dubois, Chem. Eng. Sci. 65 (2010) 261-266.
- [49] P. Darabi, K. Pougatch, M. Salcudean, D. Grecov, Int. J. Chem. React. Eng. 8 (2010).

## CHAPTER 5 GENERAL DISCUSSIONS AND PERSPECTIVE

The aim of this project was to optimize one of the most promising routes to produce value added chemicals from C5 sugars (xylose) through heterogeneous catalysis. All the chemistry happens in a single vessel. The main advantage of heterogeneous catalysis is the elimination of multiple processing steps. The conditioning of the feed stream is minimal and the excellent temperature uniformity in a fluidized bed minimizes thermal decomposition associated with sugar evaporation increasing the potential of high yields. D-xylose reacts to form maleic anhydride and acrylic acid and acrolein above 300 °C. In this process vanadyl pyrophosphate was both active and selective for maleic and acrylic acid. Acid and acrolein yield approach 50 % at 300 °C with a 3 %<sub>wt</sub> xylose solution. Gas-solid fluidized beds provide excellent heat transfer and mass transfer. Vapourizing and reacting carbohydrates (xylose) has the following advantages and limitations:

Advantages:

- (1) Higher throughput rates – higher reaction rates;
- (2) Lower catalyst inventory;
- (3) Smaller reaction vessels;
- (4) Higher selectivity;
- (5) Lower yield losses (versus fermentation, which might be as high as 50%);
- (6) Fewer unit operations;
- (7) Superior economics;
- (8) Produces specialty chemicals rather than alcohols;
- (9) Ability to react pentose sugars directly (currently extremely uncommon for fermentation processes); and,
- (10) Fewer process steps (for example, to make maleic anhydride from sugars, one must make butanol first, which is still in the development stages – (Oh-Kita & Kita, 1988)).

Limitations:

- (1) Yield needs to be higher;
- (2) Contacting liquid with the solids could form agglomerates if the solids are hydrophilic;
- (3) Vapourizing the entire liquid solution increases operational costs;
- (4) High sugar concentrations are preferred to minimize cost to vapourize the feed gas;
- (5) A more selective catalyst is required to reduce by-product acid production;
- (6) VPP catalyst agglomerates at low temperatures and high xylose aqueous mass fraction;

- (7) Increasing the temperature of the sugar solutions to these high reaction temperatures results in significant yield losses; and,
- (8) Heating the solution would cause severe operational difficulties – line blockage, deposition, coking etc.

## CHAPTER 6 CONCLUSION AND RECOMMENDATIONS

### 6.1 Conclusions

This research program was related to production of highly valued value added chemicals from C5 sugars through heterogeneous catalysis. We demonstrate that the conversion of xylose to various organic carboxylic acids can be achieved by selecting the proper catalysts and conditions, which could provide a renewable platform for the chemical industry. Due to the extremely high heat and mass transfer rates in fluidized beds, sugar evaporates and reacts catalytically faster than the homogeneous caramelization reaction. The current work concentrated on gas-phase catalytic heterogeneous partial oxidation. Vanadyl pyrophosphate is an active and selective oxidative catalyst for conversion of xylose to organic acids in the gas phase at reaction temperatures of about 300 °C. The operating conditions have a considerable effect on the product acid distribution and also the production rates. All the xylose reacts: maleic anhydride, acrylic acid and acrolein and carbon dioxide were the major compounds detected. Among the carboxylic acids, acrylic acid was the most desirable, but maleic acid was the most abundant. The highest yield for maleic anhydride was at 350 °C and for acrylic acid and acrolein it was at 300 °C. TGA tests confirmed that VPP catalyst was free of coke with a ~ 2 % weight gain. The fluidized bed operated adequately with minimal agglomeration. Furthermore, caramelization of the xylose was undetected. Liquid line blockage, agglomeration of solid catalyst inside the bed and at the tip of the injector was a challenge which was solved using gas-assisted atomization. The quality of liquid spray had significant impact on elimination of agglomeration at the bed and injector tip and products yield.

### 6.2 Recommendations

The reaction conditions need to be optimized to achieve high production rates of desired acids. More studies should be undertaken to improve atomizing the liquid feed at the micro scale. By addition of another nitrogen gas surrounding the injector tip (using both an internally mixed injector and an externally mixed injector), spray performance will improve, the sparger tip will remain clear, and there would not be any nozzle blockage and catalyst agglomeration with the periodic regeneration step for maintaining catalytic activity. Multiple injectors inside the bed

would be required if we cannot go higher than 3 %<sub>wt</sub> xylose. Changing pre-heating temperature of injected liquid should be considered in this process. Testing different metal oxide catalysts (more selective catalysts), different classes of VPO catalyst (changing the acidity of the catalyst) and also molecular sieve catalysts could be considered in future work.

I firmly believe that conducting these experiments at a larger scale will increase the product yield; in order to use larger nozzle size for liquid atomization, to carry experiments in different residence times, to inject liquid to different amount of catalyst and to re-use the capillary injector line and to atomize the xylose with higher mass fraction concentration.

## REFERENCES

Abdel-Rahman, M. A., Tashiro, Y., & Sonomoto, K. (2011). Lactic acid production from lignocellulose-derived sugars using lactic acid bacteria: overview and limits. *Journal of Biotechnology*, 156(4), 286-301.

Alen, R., Haimi, P., Heikkila, H., Koivikko, H., Nurmi, J., Ojamo, H., . . . Tylli, M. (2003). *Patent WO2002088155 A1*.

Anellotech. <http://www.anellotech.com/>

Antal Jr, M. J., Leesomboon, T., Mok, W. S., & Richards, G. N. (1991). Mechanism of formation of 2-furaldehyde from d-xylose. *Carbohydrate Research*, 217(0), 71-85.

Arena, B. J. (1983). *US Patent US 4401823 A*.

Arena, B. J., & Schumacher, E. F. (1992). *US Patent US5109128 A*.

Batis, N. H., Batis, H., Ghorbel, A., Vedrine, J. C., & Volta, J. C. (1991). Synthesis and characterization of new VPO catalysts for partial n-Butane oxidation to maleic anhydride. *Journal of Catalysis*, 128(1), 248-263.

Beall, D. S., Ohta, K., & Ingram, L. O. (1991). Parametric studies of ethanol production form xylose and other sugars by recombinant *Escherichia coli*. *Biotechnology and Bioengineering*, 38(3), 296-303.

Beatty, C., Potochnik, S., & Pease, G. (2009). *US Patent US 20090275098 A1*.

Benabdelouahab, G. F., Volta, J. C., & Olier, R. (1994). New insights into VOPO<sub>4</sub> phases through their hydration. *Journal of Catalysis*, 148(1), 334-340.

Bergman, R. I., & Frisch, N. W. (1966). *Patent US 3293268 A*.

Bernhauer, K., & Riedl-Tumova, E. (1949). Oxidation by Acetobacter. 10. Oxidation of enantiomeric forms of xylose and arabinose. *Biochemische Zeitschrift*, 321(1), 26-30.

Bi, H. T., Ellis, N., Abba, I. A., & Grace, J. R. (2000). A state-of-the-art review of gas-solid turbulent fluidization. *Chemical Engineering Science*, 55(21), 4789-4825.

Bielański, A., Piwowarczyk, J., & Poźniczek, J. (1988). Catalytic activity of vanadium oxides in the oxidation of benzene. *Journal of Catalysis*, 113(2), 334-340.

Biermann, C. J. (1996). *Handbook of pulping and papermaking*: Academic press.

Binder, J. B., Blank, J. J., Cefali, A. V., & Raines, R. T. (2010). Cover Picture: Synthesis of Furfural from Xylose and Xylan (ChemSusChem 11/2010). *ChemSusChem*, 3(11), 1209-1209. doi: 10.1002/cssc.201090043

BiofuelsDigest. <http://www.biofuelsdigest.com/>

Blommel, P. G., Yuan, L., Van Straten, M., Lyman, W., & Cortright, R. D. (2013). *US Patent US20130131411 A1*.

Bonrath, W., & Fischesser, J. (2010). *US Patent US20100217017 A1*.

Bordes, E. (1987). Crystalllochemistry of VPO phases and application to catalysis. *Catalysis Today*, 1(5), 499-526.

Bordes, E. (1988). Reactivity and crystal chemistry of V-P-O phases related to C4-hydrocarbon catalytic oxidation. *Catalysis Today*, 3(2–3), 163-174.

Bordes, E. (1993). Nature of the active and selective sites in vanadyl pyrophosphate, catalyst of oxidation of n-butane, butene and pentane to maleic anhydride. *Catalysis Today*, 16(1), 27-38.

Bordes, E., & Courtine, P. (1979). Some selectivity criteria in mild oxidation catalysis: VPO phases in butene oxidation to maleic anhydride. *Journal of Catalysis*, 57(2), 236-252.

Brown, P. (1961). Utilization of d-and l-xylose by twenty species of bacteria. *Bios* (vol. 32, p. 77-81).

Bruhns, S., & Werther, J. (2005). An investigation of the mechanism of liquid injection into fluidized beds. *AICHE Journal*, 51(3), 766-775.

Buchert, J., Viikari, L., Linko, M., & Markkanen, P. (1986). Production of xylonic acid by *pseudomonas fragi*. *Biotechnology Letters*, 8(8), 541-546.

Bugrayev, A., Al-Haq, N., Okopie, R. A., Qazi, A., Suggate, M., Sullivan, A. C., & Wilson, J. R. (2008). Covalently linked ethylmercaptophenyl sulfonic acid and ethylmercaptobenzyl sulfonic acid silica materials—Synthesis and catalytic activity. *Journal of Molecular Catalysis A: Chemical*, 280(1), 96-101.

Busca, G., Centi, G., Trifiro, F., & Lorenzelli, V. (1986). Surface acidity of vanadyl pyrophosphate, active phase in n-butane selective oxidation. *Journal of Physical Chemistry*, 90(7), 1337-1344.

Casey, J. P. (1980). Pulp and paper chemistry and chemical technology: John Wiley and Sons. New York.

Cavani, F., Mazzoni, G., & Stefani, G. (1998). *US Patent US 5847163 A*.

Centi, G. (1993). Vanadyl pyrophosphate - a critical overview. *Catalysis Today*, 16(1), 5-26.

Centi, G., Golinelli, G., & Busca, G. (1990). Modification of the surface pathways in alkane oxidation by selective doping of Broensted acid sites of vanadyl pyrophosphate. *Journal of Physical Chemistry*, 94(17), 6813-6819.

Centi, G., Trifiro, F., Ebner, J. R., & Franchetti, V. M. (1988). Mechanistic aspects of maleic anhydride synthesis from C4 hydrocarbons over phosphorus vanadium oxide. *Chemical Reviews*, 88(1), 55-80.

Chheda, J. N., Huber, G. W., & Dumesic, J. A. (2007). Liquid-phase catalytic processing of biomass-derived oxygenated hydrocarbons to fuels and chemicals. *Angewandte Chemie International Edition*, 46(38), 7164-7183.

Comotti, M., Pina, C. D., Matarrese, R., Rossi, M., & Siani, A. (2005). Oxidation of alcohols and sugars using Au/C catalysts: Part 2. Sugars. *Applied Catalysis A: General*, 291(1), 204-209.

Congress, U. (2000). *Biomass research and development act of 2000*. Communication présentée à US Congress, Washington, DC.

Contractor, R. M., Bergna, H. E., Chowdhry, U., & Sleight, A. W. (1989). Attrition resistant catalyst for fluidized bed systems. *Fluidization VI* (p. pp. 589-596). New-York: Engineering Foundation.

Contractor, R. M., Bergna, H. E., Horowitz, H. S., Blackstone, C. M., Chowdhry, U., & Sleight, A. W. (1988). Butane oxidation to maleic anhydride in a recirculating solids reactor. J. W. Ward (Édit.), *Studies in Surface Science and Catalysis* (vol. Volume 38, p. 645-654): Elsevier.

Cornaglia, L. M., Lombardo, E. A., Andersen, J. A., & Fierro, J. L. G. (1993). Acidity and catalytic behavior of vanadium-phosphorus-oxygen catalysts. *Applied Catalysis A: General*, 100(1), 37-50.

Cortright, R. D. (2013). *US Patent US7767867 B2*.

Cortright, R. D., & Blommel, P. G. (2013). *US Patent US8053615 B2*.

Courtine, P., & Bordes, E. (1997). Mode of arrangement of components in mixed vanadia catalyst and its bearing for oxidation catalysis. *Applied Catalysis A: General*, 157(1), 45-65.

Crabtree, S., & Tyers, D. (2007). *US Patent US20070123739 A1*.

Deller, K., Despeyroux, B., Krause, H., & Peldszus, E. (1992). Method for preparation of gluconic acid by catalytic oxidation of glucose: Google Patents.

Drochner, A., Kampe, P., Menning, N., Blickhan, N., Jekewitz, T., & Vogel, H. (2014). Acrolein Oxidation to Acrylic Acid on Mo/V/W-Mixed Oxide Catalysts. *Chemical Engineering & Technology*, 37(3), 398-408. doi: 10.1002/ceat.201300797

El Khadem, H. S., Ennifar, S., & Isbell, H. S. (1987). Contribution of the reaction pathways involved in the isomerization of monosaccharides by alkali. *Carbohydrate Research*, 169 13-21.

Engelskirchen, K., Fischer, H., Juettner, W., Moeller, T., & Verholt, H.-W. (1998). *US Patent US5821360 A*.

Fan, L.-S. (2011). *Chemical looping systems for fossil energy conversions*: John Wiley & Sons.

Fengel, D., & Grosser, D. (1975). Chemische Zusammensetzung von Nadel- und Laubhölzern. *HOLZ als Roh- und Werkstoff*, 33(1), 32-34.

Fiorentino, M., Newton, D., Salem, G., & Williams, B. (2003). Oxidation process in fluidised bed reactor: Google Patents.

Fuente-Hernández, A., Corcos, P.-O., Beauchet, R., & Lavoie, J.-M. (2013). Biofuels and co-products out of hemicelluloses.

Geldart, D. (1973). Types of gas fluidization. *Powder technology*, 7(5), 285-292.

Governo, A., Proenca, L., Parpot, P., Lopes, M., & Fonseca, I. (2004). Electro-oxidation of D-xylose on platinum and gold electrodes in alkaline medium. *Electrochimica Acta*, 49(9), 1535-1545.

Grzybowska, B. (1987). The vanadia-titania system in oxidation reactions. *Catalysis Today*, 1(3), 341-346.

Hattori, K., Ishii, M., Matsuda, M., Miya, B., Saito, H., Takizawa, H., & Watanabe, H. (1978). *US Patent US 4108891*.

Hayasida, A. (1938). Demonstration of pentose oxidase and catalase in Fusaria. *Biochemische Zeitschrift*, 298 169-178.

Heracleous, E., & Lemonidou, A. (2013). CAT4BIO conference: Advances in catalysis for biomass valorization. *Platinum Metals Review*, 57(2), 101-109.

Himmel, M. E., Vinzant, T., Bower, S., & Jechura, J. (2005). *BSCL use plan: solving biomass recalcitrance* (Report NREL/TP-510-37902). National Renewable Energy Laboratory.

Hodnett, B. K. (1987). An overview of recent developments in elucidating the mechanism of selective oxidation of C-4 hydrocarbons over vanadium phosphorus oxide catalysts. *Catalysis Today*, 1(5), 527-536.

Huber, G. W., Cheng, Y. T., Wang, Z., & Fan, W. (2013). *US Patent US20130324772 A1*.

Huber, G. W., Zhang, H., & Carlson, T. (2013). *US Patent US20130060070 A1*.

Hurd, C. D., & Isenhour, L. L. (1932). Pentose reactions. II. Derivatives of xylose. *Journal of the American Chemical Society*, 54(2), 693-698.

ICIS. <http://www.icispricing.com/>

Isbell, H. S., Frush, H. L., & Martin, E. T. (1973). Reactions of carbohydrates with hydroperoxides: Part I. Oxidation of aldoses with sodium peroxide. *Carbohydrate Research*, 26(2), 287-295.

Ishizaki, H., Ihara, T., J, Y., M, S., & Imai, T. (1973). D-xylonic acid production by enterobacter-cloacae. *Journal of the Agricultural Chemical Society of Japan*, 47(12), 755-761.

Jackson, J. E., Miller, D. J., & Marincean, S. (2008). *US Patent US20070066844 A1*.

Johansson, M., & Samuelson, O. (1977). Reducing end groups in birch xylan and their alkaline degradation. *Wood Science and Technology*, 11(4), 251-263.

Jokic, A., Ristic, N., Jaksic, M., Spasojevic, M., & Krstajic, N. (1991). Simultaneous electrolytic production of xylitol and xylonic acid from xylose. *Journal of Applied Electrochemistry*, 21(4), 321-326.

Jurewicz, A. T., Weinstein, B., & Young, L. B. (1975). *Patent US 3888886 A*.

Kamm, B., Gruber, P. R., & Kamm, M. (2007). Biorefineries – industrial processes and products. *Ullmann's Encyclopedia of Industrial Chemistry*: Wiley-VCH Verlag GmbH & Co. KGaA.

Kania, J., Blommel, P., Woods, E., Dally, B., Lyman, W., & Cortright, R. (2013). *US Patent US20130263498 A1*.

Kerr, R. O. (1964). *Patent US 3156705 A*.

Kiely, D. E., & Hash, K. R. (2008). *US Patent US20080033205 A1*.

Kim, D.-H., Kim, S.-H., & Shin, H.-S. (2009). Sodium inhibition of fermentative hydrogen production. *International Journal of Hydrogen Energy*, 34(8), 3295-3304.

Knapper, B. A., Gray, M. R., Chan, E. W., & Mikula, R. (2003). Measurement of efficiency of distribution of liquid feed in a gas-solid fluidized bed reactor. *International Journal of Chemical Reactor Engineering, 1*(1).

Kunii, D., & Levenspiel, O. (1969). *Fluidization engineering*.

Kunkes, E. L., Simonetti, D. A., West, R. M., Serrano-Ruiz, J. C., Gärtner, C. A., & Dumesic, J. A. (2008). Catalytic conversion of biomass to monofunctional hydrocarbons and targeted liquid-fuel classes. *Science, 322*(5900), 417-421.

Lachke, A. (2002). Biofuel from D-xylose - the second most abundant sugar. *Resonance, 7*(5), 50-58.

Lessard, J., Morin, J.-F., Wehrung, J.-F., Magnin, D., & Chornet, E. (2010). High yield conversion of residual pentoses into furfural via zeolite catalysis and catalytic hydrogenation of furfural to 2-methylfuran. *Topics in Catalysis, 53*(15-18), 1231-1234.

Levin, D. B., Pitt, L., & Love, M. (2004). Biohydrogen production: prospects and limitations to practical application. *International Journal of Hydrogen Energy, 29*(2), 173-185.

Li, N., Tempsett, G. A., & Huber, G. W. (2010). Green gasoline from aqueous phase hydrodeoxygenation of carbohydrate.

Mallat, T., & Baiker, A. (2004). Oxidation of alcohols with molecular oxygen on solid catalysts. *Chemical reviews, 104*(6), 3037-3058.

Mars, P., & Van Krevelen, D. W. (1954). Oxidations carried out by means of vanadium oxide catalysts. *Chemical Engineering Science, 3* 41-59.

Martín del Campo, J. S., Rollin, J., Myung, S., Chun, Y., Chandrayan, S., Patiño, R., . . . Zhang, Y. H. P. (2013). High-yield production of dihydrogen from xylose by using a synthetic enzyme cascade in a cell-free system. *Angewandte Chemie International Edition, 52*(17), 4587-4590. doi: 10.1002/anie.201300766

Mikkola, J.-P., & Salmi, T. (2001). Three-phase catalytic hydrogenation of xylose to xylitol—prolonging the catalyst activity by means of on-line ultrasonic treatment. *Catalysis today, 64*(3), 271-277.

Mikkola, J. P., Kubicka, D., Kuusisto, J., Granholm, N., Salmi, T., & Holmbom, B. (2003). Non-traditional three-phase reactor setup for simultaneous acoustic irradiation and hydrogenation. *Journal of Chemical Technology and Biotechnology, 78*(2-3), 203-207.

Miller M., J. M., McQueen S. (2005). *Energy and environmental profile of the U.S. pulp and paper industry*. Office of Energy and Efficiency and Renewable Energy: US Department of Energy.

National Renewable Energy Laboratory. <http://www.nrel.gov/biomass/biorefinery.html>

Nikolov, V., Klissurski, D., & Anastasov, A. (1991). Phthalic anhydride from o-xylene catalysis: science and engineering. *Catalysis Reviews, 33*(3-4), 319-374.

Nimlos, M. R., Blanksby, S. J., Qian, X., Himmel, M. E., & Johnson, D. K. (2006). Mechanisms of glycerol dehydration. *The Journal of Physical Chemistry A, 110*(18), 6145-6156.

Nimlos, M. R., Qian, X., Davis, M., Himmel, M. E., & Johnson, D. K. (2006). Energetics of xylose decomposition as determined using quantum mechanics modeling. *The Journal of Physical Chemistry A*, 110(42), 11824-11838.

Odebunmi, E. O., Ogunlaja, A. S., & Owalude, S. O. (2010). Kinetics of oxidation of D-arabinose and D-xylose by vanadium (V) in the presence of manganese II as homogeneous catalyst. *Journal of the Chilean Chemical Society*, 55(3), 293-297.

Oh-Kita, M., & Kita, T. (1988). *European Patent EP0168826 B1*

Okano, K., Tanaka, T., Ogino, C., Fukuda, H., & Kondo, A. (2010). Biotechnological production of enantiomeric pure lactic acid from renewable resources: recent achievements, perspectives, and limits. *Applied Microbiology and Biotechnology*, 85(3), 413-423.

Ooms, R., Dusselier, M., Geboers, J. A., de Beeck, B. O., Verhaeven, R., Gobechiya, E., . . . Sels, B. F. (2014). Conversion of sugars to ethylene glycol with nickel tungsten carbide in a fed-batch reactor: high productivity and reaction network elucidation. *Green Chemistry*, 16(2), 695-707.

Patience, G., Shekari, A., & Farrie, Y. (2013). *Patent WO2013029149 A1*.

Patience, G. S. (2013, October 28, 2013). [What can you do in a fluidized bed reactor?].

Patience, G. S., Bockrath, R. E., Sullivan, J. D., & Horowitz, H. S. (2007). Pressure calcination of VPO catalyst. *Industrial & engineering chemistry research*, 46(13), 4374-4381.

Patience, G. S., & Bordes-Richard, E. (2010). International VPO workshop: preface. *Applied Catalysis A: General*, 376(1), 1-3.

Pepera, M. A., Callahan, J. L., Desmond, M. J., Milberger, E. C., Blum, P. R., & Bremer, N. J. (1985). Fundamental study of the oxidation of butane over vanadyl pyrophosphate. *Journal of the American Chemical Society*, 107(17), 4883-4892.

Pereira, J. N., Couto, M. A. P. G., & Santa Anna, L. M. M. (2008). *Biomass of lignocelulosic composition for fuel ethanol production within the context of biorefinery*. Rio de Janeiro: Escola de Química/UFRJ: Series on Biotechnology.

Plateau, J. (1873). *Statique expérimentale et théorique des liquides soumis aux seules forces moléculaires* (vol. 2): Gauthier-Villars.

Popoff, T., & Theander, O. (1976). Reactions of D-xylose and D-glucose in alkaline, aqueous solutions. *Carbohydrate Research*, 48(1), 13-21.

Portoghese, F., Ferrante, L., Berruti, F., Briens, C., & Chan, E. (2008). Effect of injection-nozzle operating parameters on the interaction between a gas-liquid jet and a gas-solid fluidized bed. *Powder Technology*, 184(1), 1-10.

President, U. (1999). *Developing and promoting bio-based products and bioenergy*. Communication présentée à The White House, Washington, DC.

Prüsse, U., Heidkamp, K., Decker, N., Herrmann, M., & Vorlop, K. D. (2010). Veredelung nachwachsender rohstoffe durch selektivoxidation mit goldkatalysatoren. *Chemie Ingenieur Technik*, 82(8), 1231-1237.

Qian, X., Nimlos, M. R., Johnson, D. K., & Himmel, M. E. (2005). *Acidic sugar degradation pathways*. Communication présentée à Twenty-Sixth Symposium on Biotechnology for Fuels and Chemicals (p. 989-997).

Rase, H. F. (2000). Oxidation. *Handbook of commercial catalysts: Heterogeneous catalysts* (p. 282-287): CRC press.

Regalbuto, J. R. (Jun 25 2009). *Green Gasoline at NSF*. Communication présentée à ACS Green Chemistry and Engineering Conference, University Park, MD.

Riihimaeki Teppo, G. M., Tylli Matti, Heikkilae Heikki, Kuusisto Jyrki. (2006). *UK Patent 2437517-A*.

Saladino, R., & Farina, A. (2013). *US Patent US8609895 B2*.

Shapley, P. (2012). Oxidation reactions of sugars  
<http://butane.chem.uiuc.edu/pshapley/GenChem2/B7/index.html>

Singh, A., & Mishra, P. (1995). *Microbial pentose utilization: current applications in biotechnology*: Elsevier.

Singh, A. K., Srivastava, S., Srivastava, J., & Singh, R. (2007). Kinetics and mechanism of the Ir (III)-catalyzed oxidation of xylose and maltose by potassium iodate in aqueous alkaline medium. *Carbohydrate Research*, 342(8), 1078-1090.

Soares, A. P. V., Portela, M. F., & Kiennemann, A. (2005). Methanol selective oxidation to formaldehyde over iron-molybdate catalysts. *Cataly. Rev.*, 47(1), 125-174.

Sovani, S., Sojka, P., & Lefebvre, A. (2001). Effervescent atomization. *Progress in Energy and Combustion Science*, 27(4), 483-521.

Stevens, J. G., Bourne, R. A., Twigg, M. V., & Poliakoff, M. (2010). Real-time product switching using a twin catalyst system for the hydrogenation of furfural in supercritical CO<sub>2</sub>. *Angewandte Chemie*, 122(47), 9040-9043.

Strutt, J. W., & Rayleigh, L. (1879). *On the instability of jets*. Communication présentée à Proc. R. Soc. London A (vol. 10, p. 4-13).

Sultan, F., Ashgriz, N., Guildenbecher, D., & Sojka, P. (2011). Electrosprays. *Handbook of Atomization and Sprays* (p. 727-753): Springer.

Sun, J., & Liu, H. (2011). Selective hydrogenolysis of biomass-derived xylitol to ethylene glycol and propylene glycol on supported Ru catalysts. *Green Chemistry*, 13(1), 135-142.

Suslick, K. S. (1998). *Kirk-Othmer encyclopedia of chemical technology*. Dans. New York: John Wiley and Sons, Inc.

Tandiroy, O., Gil, I., & Sanchez, O. (2009). Modeling of maleic anhydride production from a mixture of n-butane and butenes in fluidized bed reactor. *Latin American applied research*, 39(1), 19-26.

Thompson, D. T. (2006). An overview of gold-catalysed oxidation processes. *Topics in catalysis*, 38(4), 231-240.

Trifirò, F. (1993). Key properties of V-P mixed oxides in selective oxidation of C4 and C5 n-paraffins. *Catalysis Today*, 16(1), 91-98.

Van der Weijden, R., Mahabir, J., Abbadi, A., & Reuter, M. (2002). Copper recovery from copper (II) sulfate solutions by reduction with carbohydrates. *Hydrometallurgy*, 64(2), 131-146.

Vassallo, P., & Ashgriz, N. (1991). Satellite formation and merging in liquid jet breakup. *Proceedings of the Royal Society of London. Series A: Mathematical and Physical Sciences*, 433(1888), 269-286.

Védrine, J. C. (1994). *EUROCAT oxide*: Elsevier.

Venema, F. R., Peters, J. A., & van Bekkum, H. (1992). Platinum-catalyzed oxidation of aldopentoses to aldaric acids. *Journal of Molecular Catalysis*, 77(1), 75-85.

Wabnitz, T., Breuninger, D., Heimann, J., Backes, R., & Pinkos, R. (2010). *US Patent US20100099895 A1*.

Wabnitz, T., Breuninger, D., Heimann, J., Backes, R., & Pinkos, R. (2012). *US Patent US8168807 B2*.

Wagner, M. L., Kirkwood, D. W. W., & Kiyonage, K. (2000). Oxygen enrichment process for air based gas phase oxidations which use metal oxide redox catalysts: Google Patents.

Wainwright, M. S., & Foster, N. R. (1979). Catalysts, kinetics and reactor design in phthalic anhydride synthesis. *Catalysis Reviews*, 19(2), 211-292.

Werpy, T., Petersen, G., Aden, A., Bozell, J., Holladay, J., White, J., . . . Jones, S. (2004). *Top value added chemicals from biomass. Volume 1-Results of screening for potential candidates from sugars and synthesis gas* (Report No. DOE/GO-102004-1992). Office of Scientific and Technical Information: U.S. Department of Energy.

Wisniak, J., Hershkowitz, M., Leibowitz, R., & Stein, S. (1974). Hydrogenation of xylose to xylitol. *Industrial & Engineering Chemistry Product Research and Development*, 13(1), 75-79.

Wisniak, J., Hershkowitz, M., & Stein, S. (1974). Hydrogenation of xylose over platinum group catalysts. *Industrial & Engineering Chemistry Product Research and Development*, 13(4), 232-236.

Yadav, A., Chaudhari, A., & Kothari, R. (2011). Bioconversion of renewable resources into lactic acid: an industrial view. *Critical reviews in biotechnology*, 31(1), 1-19.

Yang, W.-c. (2003). *Handbook of fluidization and fluid-particle systems*: CRC Press.

Yoshitake, J., Ohiwa, H., Shimamura, M., & Imai, T. (1971). Production of polyalcohol by a corynebacterium species. I. Production of pentitol from aldopentose. *Agricultural and Biological Chemistry*, 35(6), 905-911.

Zhang, W., Zhu, Y., Niu, S., & Li, Y. (2011). A study of furfural decarbonylation on K-doped Pd/Al<sub>2</sub>O<sub>3</sub> catalysts. *Journal of Molecular Catalysis A: Chemical*, 335(1), 71-81.

Zhanglin, Y., Forissier, M., Sneeden, R. P., Védrine, J. C., & Volta, J. C. (1994). On the Mechanism of n-Butane Oxidation to Maleic Anhydride on VPO Catalysts: I. A Kinetics Study on a VPO Catalyst as Compared to VPO Reference Phases. *Journal of Catalysis*, 145(2), 256-266.

Ziolkowski, J., Bordes, E., & Courtine, P. (1990). Oxidation of butane and butene on the (100) face of  $(VO)_2P_2O_7$ : A dynamic view in terms of the crystallochemical model of active sites. *Journal of Catalysis*, 122(1), 126-150.

Zoebelein, H. (2001). *Dictionary of Renewable Resources*: Wiley-VCH Verlag GmbH.

## APPENDICES

The reaction mechanism to convert d-xylose to maleic anhydride, acrylic acid and acrolein is presented in Appendix A.

## Appendix A

Several mechanisms have been proposed to describe xylose decomposition. Furfural is the principal product. The protonation of C3 and C4 hydroxyl groups (Fig. AA-1 and Fig. AA-2) dehydrate the site and open up the molecule (Binder, Blank, Cefali, & Raines, 2010; Qian, Nimlos, Johnson, & Himmel, 2005). In the case of C3 dehydration, the chain closes back into a five member cyclic molecule. The C-OH attached to the C3 of the new molecule is attacked by a proton, the molecule dehydrates and the remaining carbon C is oxidized to form CO or CO<sub>2</sub>. The dehydration of the C2-OH is followed by the redistribution of oxygen's electrons to form a double-bond between C2 and C3. Meanwhile, the loss of the proton from C1 produces a C=O double-bond. A second C=O double bond is created by the oxidization of C4 by V(V). (VO)<sub>2</sub>P<sub>2</sub>O<sub>7</sub> catalyzes the oxidation of C4 of malic anhydride by the Mars et Van Krevelen (1954) mechanism (Zhanglin, Forissier, Sneeden, Vedrine, & Volta, 1994) to fumaric acid. Isomerization of maleic acid drives fumaric acid.

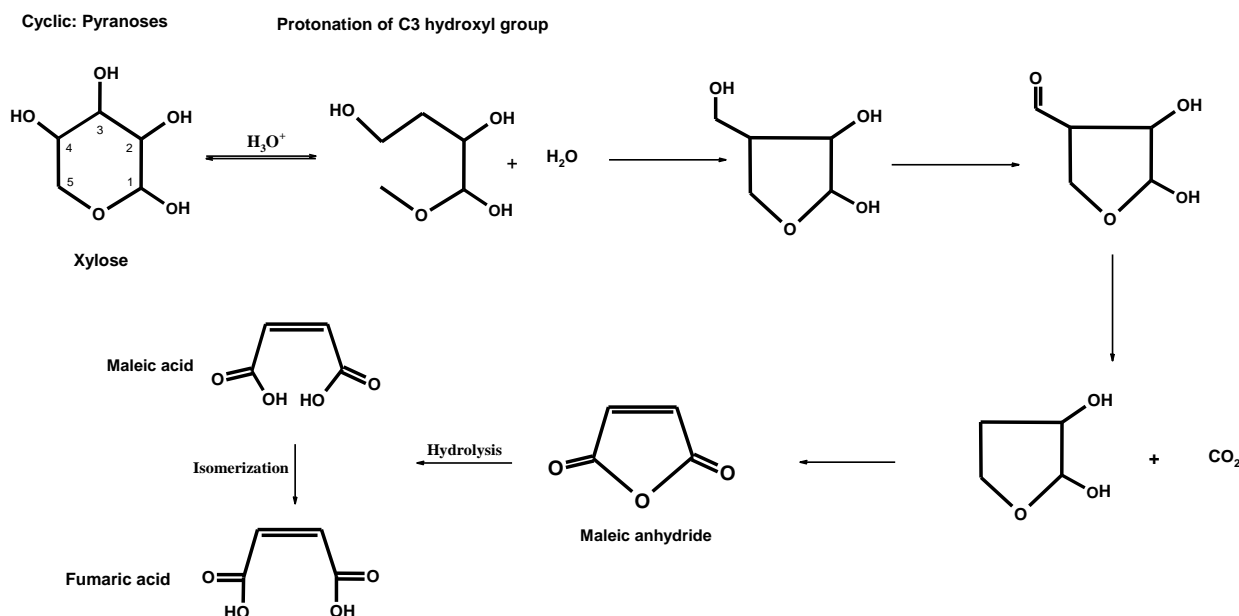


Figure AA-1: Reaction mechanism of cyclic form of d-xylose (Protonation of C3)

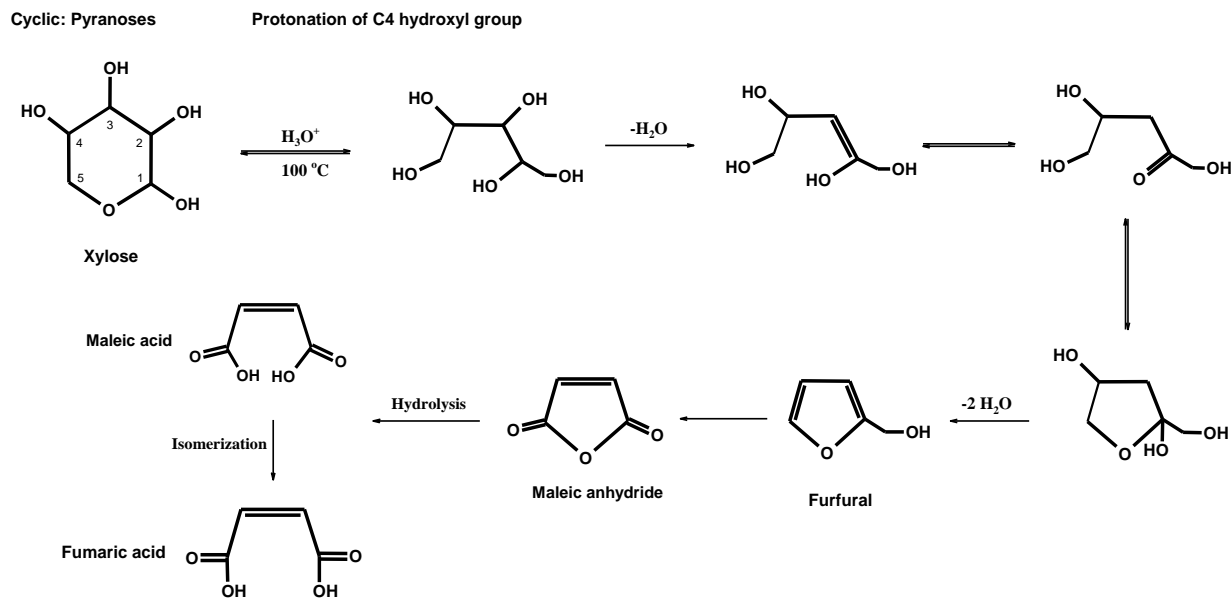


Figure AA-2: Reaction mechanism of cyclic form of d-xylose (Protonation of C4)

Another mechanism for the formation of fumaric acid was derived from quantum mechanical calculation by Nimlos, Qian, Davis, Himmel et Johnson (2006) that confirms the mechanism proposed by Antal Jr, Leesomboon, Mok et Richards (1991).

The presence of acrolein and of acrylic acid can be accounted for by the conversion of the linear form of xylose to glycerol. Ooms et al. (2014) modeled the transformation of fructose in glycerol by the retro-aldol reaction mechanism followed by hydrogenation. The same mechanism explains the break of the C2-C3 bond generated by the de-protonation of the first OH group. The reaction products are glycerol and ethanal (Fig. AA-3). Further, the acrolein is obtained from the dehydration of glycerol. Nimlos, Blanksby, Qian, Himmel et Johnson (2006) detailed this reaction mechanism from ab initio calculations. The acrylic acid is formed by partial oxidation of acrolein as is described by Drochner et al. (2014) who also used a V based catalyst.

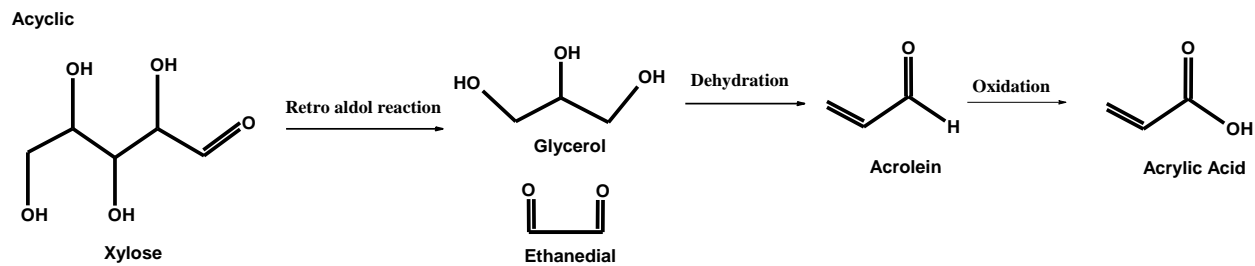


Figure AA-3: Reaction mechanism of acyclic form of d-xylose

## Appendix B

Minimum fluidization velocity of different catalyst system which is been used in this process are in the Table AB-1.

Table AB-1. Catalyst systems

Catalyst	Composition	$U_{mf}$ ( $\text{cm s}^{-1}$ )	$d_p$ ( $\mu\text{m}$ )	$\rho_p$ ( $\text{g cm}^{-3}$ )
Vanadyl pyrophosphate (VPP)	$(\text{VO})_2\text{P}_2\text{O}_7 + 10\% \text{ SiO}_2$	0.5	80	1.7
Molybdenum trioxide - cobalt oxide	$\text{MoO}_3\text{CoO}$	0.4	70	1.8
Iron molybdate	$\text{Fe}_2(\text{MoO}_4)_3$	0.7	100	1.6